MOLECULAR AND CELLULAR BIOLOGY, June 2007, p. 4526–4540 Vol. 27, No. 12
0270-7306/07/$08.00+0 doi:10.1128/MCB.01724-06


# CIF-1, a Shared Subunit of the COP9/Signalosome and Eukaryotic Initiation Factor 3 Complexes, Regulates MEL-26 Levels in the *Caenorhabditis elegans* Embryo▽

Sarah Luke-Glaser,[1] Marcia Roy,[2] Brett Larsen,[2] Thierry Le Bihan,[3] Pavel Metalnikov,[2] Mike Tyers,[2]† Matthias Peter,[1]† and Lionel Pintard[2,4]*†

*Swiss Federal Institute of Technology Zurich (ETH), Institute of Biochemistry, HPM G8, ETH Hoenggerberg, 8093 Zurich, Switzerland[1]; Samuel Lunenfeld Research Institute, Mount Sinai Hospital, 600 University Avenue, Toronto, Ontario M5G 1X5, Canada[2]; The Campbell Family Institute for Breast Cancer Research, Ontario Cancer Institute, Toronto, Ontario M5G 2M9, Canada[3]; and Institut Jacques Monod-CNRS, Université Paris VI et VII, 2 Place Jussieu Tour 43, 75251 Paris Cedex 05, France[4]*

Received 12 September 2006/Returned for modification 16 November 2006/Accepted 7 March 2007

**The *C*OP9/*sign*alosome (CSN) is an evolutionarily conserved macromolecular complex that regulates the *c*ullin-*R*ING *l*igase (CRL) class of E3 ubiquitin ligases, primarily by removing the ubiquitin-like protein Nedd8 from the cullin subunit. In the *Caenorhabditis elegans* embryo, the CSN controls the degradation of the microtubule-severing protein MEI-1 through CUL-3 deneddylation. However, the molecular mechanisms of CSN function and its subunit composition remain to be elucidated. Here, using a proteomic approach, we have characterized the CSN and CUL-3 complexes from *C. elegans* embryos. We show that the CSN physically interacts with the CUL-3-based CRL and regulates its activity by counteracting the autocatalytic instability of the substrate-specific adaptor MEL-26. Importantly, we identified the uncharacterized protein K08F11.3/CIF-1 (for *C*SN-eukaryotic *i*nitiation *f*actor 3 [eIF3]) as a stoichiometric and functionally important subunit of the CSN complex. CIF-1 appears to be the only ortholog of Csn7 encoded by the *C. elegans* genome, but it also exhibits extensive sequence similarity to eIF3m family members, which are required for the initiation of protein translation. Indeed, CIF-1 binds eIF-3.F and inactivation of *cif-1* impairs translation in vivo. Taken together, our results indicate that CIF-1 is a shared subunit of the CSN and eIF3 complexes and may therefore link protein translation and degradation.**

The protein synthesis and degradation machineries must be tightly coregulated to provide cells with the right set of proteins in their various physiological states during their entire life cycle, yet the molecular mechanisms that coordinate protein translation and degradation are still poorly understood.

The ubiquitin-proteasome system is the major nonlysosomal mechanism responsible for the degradation of intracellular proteins. In this pathway, proteins are targeted for rapid proteolysis upon conjugation to ubiquitin, a conserved protein with 76 amino acids (20). Substrate proteins are covalently linked to ubiquitin through a series of *trans*-thioesterification reactions catalyzed by an enzymatic cascade (21). The C-terminal glycine residue of ubiquitin is first thioesterified to an E1 (ubiquitin-activating) enzyme in an ATP-dependent manner; transferred to an E2 (ubiquitin-conjugating) enzyme, also as a thioester linkage; and finally, through the action of an E3 (ubiquitin ligase), transferred to a lysine residue on the substrate as an isopeptide linkage. Reiteration of the catalytic cycle is thought to assemble a polyubiquitination chain, which acts to target the substrate to the 26S proteasome (43). The proteasome consists of a core 20S cylinder and a 19S regulatory complex that caps either end of the cylinder and controls substrate entry. The regulatory complex is composed of the proteasome lid subcomplex, which processes polyubiquitinylated substrates through its deubiquitinylation activity (57), and the "base," which unfolds and threads substrates into the 20S catalytic lumen by virtue of its hexameric ring of six AAA ATPases (16).

Intriguingly, the proteasome lid subcomplex shares similarities with two other macromolecular complexes involved in protein synthesis and degradation, the eukaryotic initiation factor 3 (eIF3) complex and the COP9/signalosome (CSN). The eIF3 complex plays a central role in protein translation by promoting ribosome dissociation, binding of the initiator methionyl-tRNA to the 40S ribosomal subunit, and mRNA recruitment to the ribosome (4). The CSN, first described in plants as a regulator of photomorphogenesis (8, 59), regulates the activity of cullin-RING E3-ubiquitin ligases (CRLs), which trigger the proteasomal degradation of numerous protein substrates (42, 62).

Despite these different functions, all three complexes use several subunits harboring at their extreme C termini a PCI (for *p*roteasome-*C*SN/e*I*F3) domain (23). Other subunits of these complexes share another homology domain called MPN (for *M*pr1-*P*ad1 *N*-terminal) domain (3, 23). While PCI-containing subunits may primarily serve a structural role, some MPN subunits are catalytically active and exhibit metalloprotease activity (11, 57).

The proteasome lid and the CSN are composed of eight core

* Corresponding author. Mailing address: Institut Jacques Monod-Centre National de la Recherche Scientifique, Université 6 et 7, 2, place Jussieu Tour 43, 75251 Paris Cedex 05, France. Phone: (33)-1-44-27-77-98. Fax: (33)-1-44-27-52-65. E-mail: pintard.lionel@ijm.jussieu.fr.

† Mike Tyers, Matthias Peter, and Lionel Pintard contributed equally to this study.

▽ Published ahead of print on 2 April 2007.

subunits, six of the PCI and two of the MPN class. Each subunit of the proteasome lid contains a paralogue in the CSN complex, so that there is a direct one-to-one correspondence between their subunits. In addition, both complexes may assemble into similar ring-shaped structures, with each paralogue located in exactly the same position within the ring (26). In contrast, the eIF3 complex contains at least 12 subunits. Similarly to the CSN and the proteasome lid, the eIF3 complex harbors two MPN subunits, which, however, lack the residues typically found in metalloproteases and are thus catalytically inactive. The total number of PCI subunits in the eIF3 complex remains to be defined, and there is currently no information on the structural organization of the complex.

We are interested in the function and regulation of CRLs. In these complexes, the cullin subunit functions as a platform that bridges one of many substrate recognition subunits to the common RING finger protein Rbx1, which in turn recruits the E2 enzyme that provides catalytic activity (62, 67). Yeast genomes encode only three cullins, while the genomes of higher eukaryotes encode six or seven cullins (28). Each family of cullins assembles an active E3 ligase containing Rbx1 but uses a distinct substrate recognition module (42). This module is constituted either of heterodimers composed of an adaptor subunit and a substrate binding protein (e.g., Skp1/F-box protein in CRL1 or elongin C/VHL box protein in CRL2) or a single protein that merges the two functions (e.g., BTB adaptor protein in CRL3). In most cases, the adaptor binds the N-terminal part of the cullin through a BTB (for *b*ric-à-brac, *t*ramtrack, *b*road complex) fold (42, 45, 62). The only adaptor that does not contain such a domain is DDB1, which links Cul4 to the numerous Decaf proteins that function as substrate recruitment factors (2, 25). In *Caenorhabditis elegans*, the CUL-3-based ubiquitin ligase regulates the meiosis-to-mitosis transition of fertilized embryos by triggering the degradation of MEI-1 (for *mei*osis defective 1)/katanin (6). MEI-1 is a microtubule-severing protein of the AAA ATPase family essential for the assembly of the meiotic spindle (52, 53). However, its persistence during the following mitosis, as observed in *cul-3*(*RNAi*) embryos or embryos expressing a gain-of-function allele [*mei-1(ct46)*], is highly toxic, leading to severe defects in microtubule-dependent processes (9, 31, 44). Within the CUL-3 complex, the autocatalytically unstable BTB adaptor MEL-26 (for *m*aternal *e*ffect *l*ethal 26) specifically recognizes MEI-1 (13, 46, 64).

All cullin family members are modified by covalent linkage of the ubiquitin-like protein Nedd8 to a conserved lysine residue located at the C terminus next to the Rbx1 binding site (24). Nedd8 conjugation is catalyzed by an E1-like heterodimer (Ula1/Uba3) that transfers activated Nedd8 to a dedicated E2 enzyme, Ubc12 (32, 35), while the evolutionarily conserved protein Dcn1 may be the long-sought Nedd8 E3 ligase (30). Neddylation is essential in all species except budding yeast (32, 35). Counteracting the neddylation pathway, the CSN regulates CRL activity by hydrolyzing the cullin-Nedd8 conjugate (39, 49). Several lines of evidence indicate that the Csn5 subunit, which bears a JAMM/metalloprotease domain, promotes cullin deneddylation (11). While the CSN appears to inhibit CRL activity in vitro, genetic analysis has revealed an essential role of this complex in MEI-1 degradation in vivo. Indeed, both neddylation and deneddylation of CUL-3 are essential to target MEI-1 for ubiquitin-mediated degradation after meiosis (44). Intriguingly, reducing CSN function suppresses partial inactivation of the neddylation pathway, suggesting that the balance between neddylation and deneddylation is essential for CUL-3 activity. NED-8 modification may promote CRL assembly through dissociation of the cullin scaffold from the inhibitor CAND1 (37, 66) and/or stimulate CUL-3-based ligase function by facilitating the recruitment of the E2 enzyme (27). However, the precise role of the CSN in MEI-1 degradation is currently unknown. Moreover, the composition of this complex in *C. elegans* remains to be defined.

Here, we demonstrate that the CSN regulates the activity of the CUL-3-based E3 ligase by counteracting the autocatalytic instability of its substrate-specific adaptor, MEL-26, most likely by promoting CUL-3 deneddylation. Moreover, we report the first biochemical identification of the CSN complex in *C. elegans* embryos. We have used sensitive liquid chromatography-mass spectrometry/mass spectrometry (LC-MS/MS) analysis of immunopurified CSN and CUL-3 complexes and identified the uncharacterized PCI domain subunit K08F11.3, which we named CIF-1 (for *C*SN-e*IF*3 1). CIF-1 appears to be the only ortholog of Csn7 encoded by the *C. elegans* genome, but it also exhibits extensive sequence similarity to eIF3m family members. Importantly, our results indicate that CIF-1 is functionally shared between the CSN and the eIF3 complex, implying that in *C. elegans*, the translation and degradation machineries may be tightly coupled. We thus propose that the CSN and the eIF3 complex cooperate to maintain MEL-26 protein levels and likely other proteins in *C. elegans*.

## MATERIALS AND METHODS

**Recombinant DNA work.** Plasmids are listed in Table 1. Details of plasmid constructions are available upon request. Standard procedures were used for recombinant DNA manipulations (48) and the Gateway recombination-based cloning system (Invitrogen). To generate the two-hybrid constructs, cDNAs were amplified by PCR from a cDNA library (Invitrogen) and inserted in the yeast two-hybrid vectors containing the GAL4 activation domain (pACT-2) (GAL4 DNA-AD *LEU2* $Amp^r$ hemagglutinin epitope tag; 8.1 kb; Clontech), as well as in the plasmid containing the GAL4 DNA binding domain (pAS2-1) (GAL4 DB *TRP1* $Amp^r$ $CYH^s2$; 8.4 kb). Human GA17 and Csn7a were PCR amplified, cloned by Gateway into the entry vector pDONR 201 (Invitrogen), and then transferred into the destination vector [pMX-pie pDEST $(FLAG)_3$]. Human eIF3e cloned into pDONR 223 was obtained from Open Biosystems.

***C. elegans* strains and manipulations.** The *C. elegans* isolate N2 Bristol was used as the wild type, and all manipulations followed standard conditions (7). The strains VC861 {*csn-5*(*ok1064*) IV/nT1[qIs51](IV;V)}, RB1260 {*csn-2*(*ok1288*) I/hT2[bli-4(e937) let-?(q782) qIs48] (I;III)}, and VC1146 {*csn-6*(*ok1604*) IV/nT1[qIs51] (IV;V)} were provided by the Gene Knockout Consortium (http://www.celeganskoconsortium.omrf.org). *csn-2*(*ok1288*), *csn-5*(*ok1064*), and *csn-6*(*ok1604*) homozygous (green fluorescent protein [GFP] negative) and heterozygous (GFP positive) animals were manually picked under a dissecting microscope equipped with GFP fluorescence. *C. elegans* development after inhibition of protein translation was tested by growing animals at the first larval stage (L1) on nematode growth medium (NGM) plates containing 50 μg/ml of cycloheximide (CHX) (Sigma). To test CHX hypersensitivity, wild-type L4 larvae were fed for 30 h at 16°C on control bacteria or bacteria expressing double-stranded RNA (dsRNA) to partially deplete *eIF-3.a* or *cif-1* (0.5 mM IPTG [isopropyl-β-D-thiogalactopyranoside]) in the presence or absence of low doses of CHX (5 μg/ml). Five animals from each plate were then transferred to regular OP50 plates. After 7 hours, animals were removed, and the viability of their progeny was determined after 24 h.

**RNA-mediated interference.** RNA interference (RNAi) was performed by injecting *cif-1* or *cul-3* dsRNA into L4 larvae or young adults or by feeding L1 larvae on NGM plates containing 2 mM IPTG (Sigma). The construct to generate *cul-3* dsRNA was described previously (46). *cif-1* dsRNA was generated by amplifying the first 750 base pairs of the gene. *eif-3* RNAi constructs were obtained from the Ahringer laboratory.

TABLE 1. Plasmids used in this study

| Plasmid | Insert | Source or reference |
|---|---|---|
| cDNA library | | Invitrogen |
| pACT-2 | | Clontech |
| pAS2-1 | | Clontech |
| pAS2-1 | CIF-1 | This study |
| pACT-2 | CSN-1 | 44 |
| pACT-2 | CSN-2 | 44 |
| pACT-2 | CSN-3 | 44 |
| pACT-2 | CSN-4 | 44 |
| pACT-2 | CSN-5 | 44 |
| pACT-2 | CSN-6 | 44 |
| pACT-2 | CIF-1 | This study |
| pACT-2 | eIF-3.C | This study |
| pACT-2 | eIF-3.F | This study |
| pMAL-c2 | MBP | NEB |
| pLP228 | MBP–CUL-3 | This study |
| pLP251 | MBP–CSN-2 | This study |
| pLP229 | MBP–CSN-5 | This study |
| L4440 (feeding vector) | | |
| pLP36 (feeding vector) | *cul-3* | 31 |
| pLP258 (feeding vector) | *cif-1* + *csn-5* | This study |
| pLP259 (feeding vector) | *cif-1* | This study |
| pFAST Bac1 | | Invitrogen |
| pLP306 | FLAG–MEL-26 | This study |
| pDONR 201 | | Invitrogen |
| pDONR 201 | Csn7a | This study |
| pDONR 201 | GA17 | This study |
| pDONR 223 | eIF3e | Open Biosystems |
| pMX-pie pDEST (FLAG)3X | | This study |
| pMX-pie pDEST (FLAG)3X | eIF3e | This study |
| pMX-pie pDEST (FLAG)3X | GA17 | This study |
| pMX-pie pDEST (FLAG)3X | Csn7a | This study |

**HEK 293T cell culture and stable cell line selection.** Human embryonic kidney (HEK) 293T cells were grown in Dulbecco's modified Eagle high-glucose medium supplemented with 10% fetal bovine serum, 2 mM L-glutamine, and 1× antibiotic-antimycotic (Gibco). To generate stable cell lines, HEK 293T cells were transfected in 10-cm plates with 2 μg of plasmid DNA using Effectene (QIAGEN) reagent according to the manufacturer's instructions. Thirty-six hours posttransfection, the cells were trypsinized and plated into selection medium (Dulbecco's modified Eagle high-glucose medium supplemented with 10% fetal bovine serum, 2 mM L-glutamine, 1× antibiotic-antimycotic, and 1 μg/ml puromycin [InvivoGen]). The selection medium was replaced every 2 to 3 days until isolated colonies appeared. For each construct, 5 to 10 isolated colonies were picked and individually amplified. Stable cell lines were maintained for 2 weeks in culture under selective conditions before expression testing was performed as follows. Clones of stable cell lines were lysed in plates with 500 μl of lysis buffer (CLB3: 0.1% NP-40, 50 mM Tris-Cl, pH 7.5, 100 mM NaCl, 5 mM EDTA, 5 mM NaF, 10% glycerol supplemented with 1 mM dithiothreitol [DTT], 1 μg/μl leupeptin/pepstatin A, 10 μg/μl aprotinin, 100 μg/μl phenylmethylsulfonyl fluoride, and 0.2 mM $NaVO_3$) for 5 min on ice. Detergent-insoluble material was removed by centrifugation at ~18,000 × *g* in a microcentrifuge, and the protein concentration of the cleared lysates was determined using the Bio-Rad DC protein assay (Bio-Rad). Equal amounts of each cleared cell lysate were separated by sodium dodecyl sulfate-polyacrylamide gel electrophoresis (SDS-PAGE), transferred to a nitrocellulose membrane, and subsequently immunoblotted with anti-FLAG-M2 antibodies (Sigma).

**Protein extracts, antibodies, and immunoblotting.** Standard procedures were used (48). Antibodies directed against the following polypeptides were used in this study: anti-FLAG (Sigma), -MEI-1 (46), -MEL-26 (46), -CUL-3 (44), -CSN-5 (44), -CSN-2 (this study), and -eIF3 antibodies (a generous gift from J. Hershey [40]). Anti-CSN-2 polyclonal antibodies were raised against full-length CSN-2 produced and purified from *Escherichia coli* as a glutathione *S*-transferase (GST) fusion protein essentially as described previously (44). CSN-2, CSN-5, and CUL-3 antibodies were affinity purified over MBP–CSN-2, CSN-5, and CUL-3 affinity columns, respectively. To prepare the affinity columns, proteins were expressed in bacteria, purified over amylose resin according to the manufacturer's instructions (New England BioLabs), and covalently linked to CNBr-activated Sepharose (Pharmacia). The antibodies were then cross-linked to Ultralink Protein G beads (Pierce) using 20 mM of dimethylpimelimidate (Sigma) in 100 mM sodium borate buffer, pH 9. Secondary antibodies conjugated to peroxidase were purchased from Amersham.

**Protein extraction, immunopurifications, coimmunoprecipitation, and gel filtration experiments.** N2 worms were grown in liquid culture in a 35-liter fermentor essentially as described previously (47), collected by sedimentation, and bleached by hypochlorite treatment. Embryos were collected, washed several times in M9 buffer, and snap-frozen in liquid nitrogen. The embryos were then resuspended in 5 volumes of extraction buffer (buffer E: 20 mM HEPES, 150 mM NaCl, 2 mM $MgCl_2$, 10 mM EDTA, 1 mM DTT containing protease inhibitors [EDTA-free "Complete" mix from Roche]) and phosphatase inhibitors (1 mM sodium pyrophosphate, 1 mM sodium orthovanadate, 1 mM beta-glycerophosphate, 1 mM EGTA, 100 mM NaF) and ground in liquid nitrogen using a mortar and pestle. Protein extract was cleared by centrifugation three times for 10 min each time at 20,000 × *g* and 4°C. The protein concentration of the extract was determined using the Bio-Rad kit assay.

For gel filtration analysis, the extract was loaded onto a 24-ml bed gel filtration column that was equilibrated with buffer E as defined above (Superose 6; Pharmacia) at 0.3 ml/min. Then, 13 1-ml fractions were collected, and the proteins were precipitated with trichloroacetic acid (TCA)-deoxycholate, washed three times with acetone, and analyzed by Western blotting to detect CSN-2, CSN-5, and CUL-3.

For immunopurification experiments, the extract was incubated for 2 h at 4°C with affinity-purified antibodies (CSN-2, CSN-5, or CUL-3) cross-linked to Ultralink Protein G beads as described above. The beads were washed five times with buffer E. Bound proteins were eluted twice for 20 min each time at 50°C in 1 bead volume of 2× gel sample buffer without reducing agent. DTT was then added, and the eluted proteins were separated by SDS-PAGE (10%).

For immunopurification experiments from mammalian cells, HEK 293T stable cell lines were grown in five 15-cm dishes containing 30 ml of selection medium (see above). The cells were placed on ice; washed twice with ice-cold 1× Dulbecco's phosphate-buffered saline, pH 7.4 (Gibco); scraped into 2 ml of lysis buffer (CLB3); and incubated for 30 min at 4°C. Detergent-insoluble material was removed by centrifugation (two times for 20 min each time at ~30,000 × *g* and 4°C). The protein concentration of the clarified extract was determined using the Bio-Rad DC protein assay. Extracts were then incubated with 30 μl of anti-FLAG-M2 agarose beads (Sigma) for 5 h at 4°C with end-over-end rotation. The beads were washed three times with CLB3 and once with Tris-buffered saline (50 mM Tris-Cl, pH 7.5, 100 mM NaCl) containing protease inhibitors.

For SDS-PAGE–LC-MS/MS analysis, bound proteins were eluted twice by incubating beads for 45 min at 4°C in 150 μl of 150-ng/μl FLAG peptide in Tris-buffered saline. The eluates were then combined, TCA/deoxycholate precipitated, resuspended in 30 μl of 2× SDS-PAGE sample loading buffer, and separated by SDS-PAGE (10%). The gels were stained with GelCode colloidal Coomassie blue reagent (MJS BioLynx, Inc.).

For "gel-free" LC-MS/MS analysis, bound proteins were eluted twice by nutating beads for 15 min at 4°C in 50 μl of 50 mM phosphoric acid, pH 2.8. The eluates were then combined and centrifuged for 5 min at 800 × *g* to remove excess immunoglobulin G (IgG).

**Tandem mass spectrometry LC-MS/MS.** Protein gel bands were excised and trypsin digested using a ProMS digestion robot (Genomic Solutions). The resulting samples were loaded onto a 75-μm column with Zorbax $C_{18}$ (Agilent) and eluted over 30 min with an Agilent 1100 CapLC coupled to a Thermo Electron LCQ Deca.

Gel-free samples were prepared and loaded onto strong cation exchange columns, reduced with DTT, alkylated with iodoacetamide, and digested with trypsin. The resulting peptides were eluted, acidified, and analyzed by LC-MS/MS with an Agilent 1100 CapLC coupled to a Thermo Electron LTQ. Samples were loaded onto a 150-μm Zorbax $C_{18}$ precolumn and separated on a 75-μm Zorbax $C_{18}$ column over 45 min.

The resulting data files were analyzed using Mascot (41) and searching against the *C. elegans* or human entries in the NCBI nr database. Proteins with more than 2 peptides above a score of 40 were accepted as confident matches. In the case of proteins smaller than 10 kDa, single-peptide matches were accepted after manual validation.

**Immunocytochemistry and microscopy.** Embryos were freeze-cracked by flipping the coverslip, immobilized on polylysine-coated slides, and fixed for 20 min in methanol at room temperature. Affinity-purified anti-MEI-1 and anti-MEL-26 antibodies were used at a dilution of 1/250 (0.2 ng/μl). Secondary antibodies were purchased from Molecular Probes. DNA was stained by Hoechst or DAPI (4′,6′-diamidino-2-phenylindole) (Sigma). Microscopy was carried out with a

Zeiss Axiovert 200 M equipped with differential interference contrast (DIC) optics and a Hamamatsu camera.

**Yeast transformations manipulations and two-hybrid screen.** Yeast Y190 (MAT*a gal4 gal80 his3 trp1-901 ade2-101 ura3-52 leu2-3 112 URA3*::*GAL lacZ LYS2*::*GAL-HIS3 cyh*) and Y187 (MATα *gal4 gal80 his3 trp1-901 ade2-101 ura3-52 leu2-3,112 URA3*::*GAL-lacZ*) (Clontech) were transformed by the lithium acetate method and handled following standard protocols (18).

**In vitro ubiquitination assays.** For the in vitro ubiquitination assays, the $BCB^{MEL-26}$ complex (GST-Cul3/Rbx1/FLAG-MEL-26) immobilized on glutathione beads (5 μl; Pharmacia) was incubated in a final volume of 20 μl with ubiquitin or methyl-ubiquitin (100 ng/μl), ubiquitin-activating enzyme (Boston Biochem; 40 ng/μl), and ubiquitin-conjugated enzyme hUbc5-c (40 ng/μl) in ubiquitination buffer (50 mM Tris-HCl [pH 7.5], 10 mM $MgCl_2$, 2 mM ATP, 50 μM DTT). Reaction mixtures were incubated at 30°C for 60 min, terminated by the addition of 1 volume of 2× SDS sample buffer, and resolved on SDS-PAGE (10%) before being immunoblotted with specific anti-FLAG antibodies.

**In vivo labeling experiment.** In vivo labeling experiments with [$^{35}$S]methionine were performed essentially as described previously (33). Equivalent numbers of wild-type larvae fed for 24 h at 16°C on control bacteria or for 48 h on bacteria expressing dsRNA to deplete *eif-3.a* or *cif-1* were collected by centrifugation, washed several times in M9 buffer (without magnesium sulfate), and incubated for 4 h 30 min at 23°C in S complete medium containing NA22 bacteria prelabeled with [$^{35}$S]methionine as described previously (33). The larvae were then washed several times with 10 ml of S complete medium, incubated with cold NA22 bacteria for an additional hour, and collected by centrifugation (5 min at 1,000 × *g*). After five washes with 15 ml of M9 buffer, the larvae were resuspended in 1 volume of 2× sample loading buffer and boiled for 10 min at 95°C. The protein concentrations of the extracts were determined using the Bio-Rad DC protein assay, and equal quantities of proteins from each extract were spotted on 0.5-$cm^2$ Whatman filters. The filters were washed twice in 20% TCA and once with acetone, dried, and transferred into a vial containing 6 ml of scintillation liquid (Ready-Safe; Beckman Coulter). The associated radioactivity was counted on an LS6500 Multipurpose Scintillation Counter (Beckman Coulter). All quantitations were performed in triplicate.

**Database searches and bioinformatics.** We used position-specific iterated Basic Local Alignment Search Tool psi-BLAST (NCBI) to search for amino acid sequence homologies (1), ClustalW (EMBnet [http://www.ch.embnet.org]) for protein alignments, and Boxshade (EMBnet) for presenting sequence alignments (55). The unrooted tree was designed with the "neighborg-joining" algorithm. The location of the PCI domain in CIF-1 was defined according to SMART (http://smart.embl-heidelberg.de).

**Protein Data Bank accession numbers.** The accession numbers of the proteins used to generate the phylogenetic tree and the multiple alignments (see Fig. 5) are as follows. Csn7 family members: Csn7a (*Homo sapiens*), 55976618; Csn7b (*H. sapiens*), 55976598; Dch7/Csn7 (*Drosophila melanogaster*), 55976624; Csn7 (*Schizosaccharomyces pombe*), 5731945; and Csn7 (*Arabidopsis thaliana*), 21593551. GA17/eIF3m family members: GA17/eIF3m (*H. sapiens*), 30802138; CG8309 (*D. melanogaster*), 21430212; CIF-1 (*C. elegans*), 17541388; CIF-1 (*C. briggsae*), 39587635; *A. thaliana* (3G02200), 30678503; *A. thaliana* (5G15610), 30685439; and eIF3m (*S. pombe*), 63054479.

## RESULTS

**The CSN counteracts the autocatalytic instability of the BTB adaptor MEL-26 in *C. elegans* embryos.** The CUL-3-specific BTB adaptor MEL-26 accumulates at the cell cortex in *C. elegans* embryos when CUL-3 or the neddylation pathway is abrogated (38, 46), causing a hypercontractile cortex with several ingressing furrows during pronuclear migration (31, 38). To determine whether the CSN was required for MEL-26 degradation, we scored the number of ingressing furrows in *csn-1*(*RNAi*) embryos. In contrast to *cul-3*(*RNAi*) embryos, the cortex of *csn-1*(*RNAi*) embryos was not hypercontractile and behaved similarly to that of *mel-26* mutant embryos (Fig. 1A), suggesting that cortical MEL-26 did not accumulate under these conditions. Indeed, while both MEI-1 and MEL-26 levels markedly increased after inactivation of *cul-3*, MEL-26 was almost undetectable in *csn-1*(*RNAi*) embryos, despite the expected accumulation of MEI-1 and neddylated forms of CUL-3. Likewise, MEL-26 was barely detectable by immunostaining in *csn-1*(*RNAi*) embryos compared to wild-type controls (Fig. 1B and C). Northern blot analysis revealed that the amounts of *mel-26* mRNA present in *cul-3*(*RNAi*) and *csn-1*(*RNAi*) embryos were comparable to that in wild-type embryos (data not shown), indicating that the regulation occurs at the posttranslational level, most likely through ubiquitin-dependent proteolysis.

**Purified Cul3/Rbx1 heterodimers polyubiquitinate MEL-26 in vitro.** To confirm this hypothesis, we devised an in vitro system and tested whether MEL-26 was autoubiquitinated by Cul3/Rbx1 heterodimers. As shown in Fig. 1D, MEL-26 was readily autoubiquitinated by the Cul3/Rbx1 ligase in vitro. Importantly, polyubiquitinated forms of MEL-26 were not detected when E1 was omitted from the reaction or when ubiquitin was replaced with the chain terminator methyl-ubiquitin (Fig. 1D). These results suggest that MEL-26 is degraded by the 26S proteasome in vivo and that the CSN counteracts the autocatalytic instability of MEL-26, most likely via CUL-3 deneddylation. Alternatively, the CSN might control MEL-26 stability by recruiting a deubiquitinating enzyme to the active complex to disassemble spuriously formed ubiquitin chains on CRL adaptors (58, 69).

**LC-MS/MS analysis of immunopurified CSN and CUL-3 complexes identifies K08F11.3/CIF-1 as a novel subunit of the CSN complex in *C. elegans* embryos.** To identify novel components and regulators of the *C. elegans* CSN complex, we generated specific polyclonal antibodies directed against the most conserved subunits, CSN-2 and CSN-5, and used these antibodies to immunopurify the CSN complex from *C. elegans* embryonic extracts. Importantly, CSN-2 and CSN-5 coimmunopurified in reciprocal experiments, whereas no interaction was detected using the preimmune serum (Fig. 2A). Since CSN-2 does not seem to interact directly with CSN-5 in *C. elegans* (Fig. 3E) (44), these results indicate that both antibodies precipitated the entire CSN complex. Immunoblotting the extract before and after immunopurification revealed that more than 70% of CSN-2 and 80% of CSN-5 were specifically captured under these experimental conditions (data not shown).

Gel filtration experiments revealed that the *C. elegans* CSN cosediments as a macromolecular complex of ~450 kDa (Fig. 3C). To determine its composition, we analyzed CSN-2 and CSN-5 immunoprecipitates from embryonic extracts by Coomassie colloidal blue staining and LC-MS/MS analysis (Fig. 2B). As expected, in addition to CSN-2 and CSN-5, we identified all previously characterized CSN subunits, including CSN-1, CSN-3, CSN-4, and CSN-6 (44). In each case, numerous unique tryptic peptides (sequence coverage, above 25%) unambiguously identified the corresponding proteins (Fig. 2C and Table 2). Importantly, CSN-5 immunoprecipitates also contained several CUL-3 peptides (sequence coverage, 13%), indicating that the CUL-3-based ligase physically interacts with the CSN (Fig. 2B and Table 2). Numerous unique peptides identified in both CSN-2 and CSN-5 immunoprecipitates corresponded to the uncharacterized protein K08F11.3, which we name here CIF-1. The extent of protein coverage suggested that CIF-1 associated stoichiometrically with the CSN complex (Fig. 2C and D and Table 2). Consistent with this possibility, CIF-1 specifically interacted with CSN-1 and CSN-4 in yeast

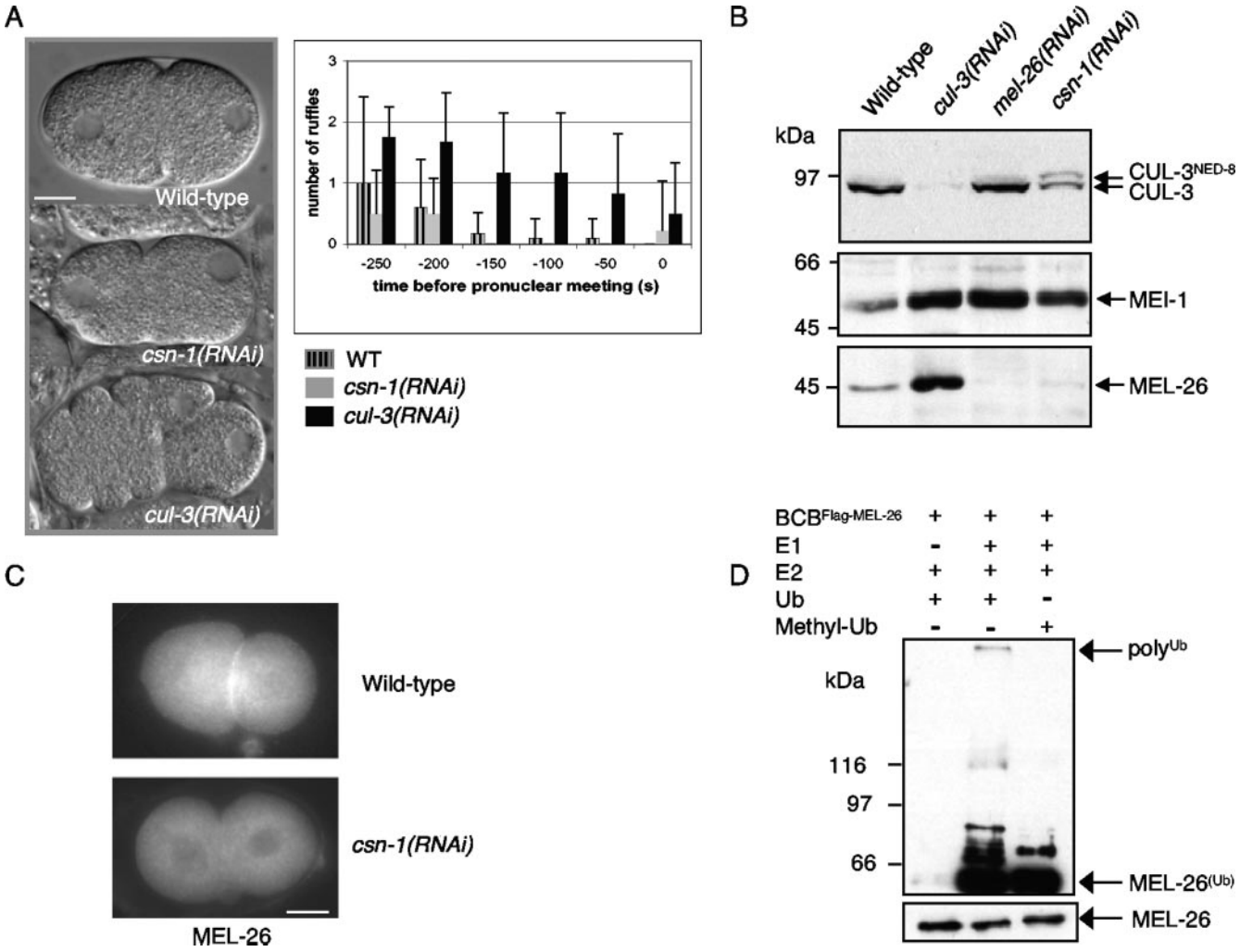


FIG. 1. The CSN counteracts the autocatalytic instability of the BTB adaptor MEL-26 in *C. elegans* embryos. (A) Analysis of cortical ruffling during pronuclear migration of (top) wild-type (WT) ($n = 5$), (middle) *csn-1*(*RNAi*) ($n = 5$), and (bottom) *cul-3*(*RNAi*) ($n = 5$) embryos by DIC microscopy. Cortical ruffling, a readout for MEL-26 accumulation, was quantified as described previously (38). The error bars represent standard deviations. The scale bar represents 10 μm. (B) Embryo extracts prepared from wild-type, *cul-3*(*RNAi*), *mel-26*(*RNAi*), and *csn-1*(*RNAi*) embryos were examined by immunoblotting them with anti-CUL-3 (top), anti-MEI-1 (middle), and anti-MEL-26 (bottom) specific antibodies. Ponceau staining of the membrane revealed that equal amounts of protein from each genotype were loaded on the gel. (C) Micrographs of MEL-26 in fixed wild-type and *csn-1*(*RNAi*) embryos. The scale bar represents 10 μm. (D) The Cul3 complex purified from insect cells (GST-Cul3, Rbx1, and FLAG–MEL-26) was incubated with components of the ubiquitin activation pathway (E1, E2, and ubiquitin [Ub]) in the presence of ATP. After 1 hour of incubation, MEL-26 ubiquitination was analyzed by immunoblotting with FLAG antibodies. The lower part of the membrane shows unmodified MEL-26, while the upper part corresponds to ubiquitinated MEL-26 species.

two-hybrid experiments (Fig. 3D). These results strongly suggest that CIF-1 is a novel core subunit of the CSN in *C. elegans*.

Interestingly, CUL-3 was found to cosediment with the CSN complex by gel filtration analysis (Fig. 3C), and both CUL-3 and MEL-26 interacted with CSN-5 in coimmunoprecipitation experiments (Table 2). To test whether CIF-1 also copurified with CUL-3, we immunopurified CUL-3 from embryonic extracts and subjected its associated proteins to LC-MS/MS analysis (Fig. 3A and B). Peptides that corresponded to CUL-3, NED-8, and MEL-26, as well as CSN-1, CSN-5, and CIF-1, were identified by this approach (Fig. 3B and Table 2), demonstrating that the CSN complex including CIF-1 is stably associated with the CUL-3 complex.

**CIF-1 controls CUL-3 deneddylation and MEI-1 degradation in *C. elegans* embryos.** The CSN complex is required for the mitotic divisions of the one-cell stage embryo through its regulation of CUL-3 activity (44). To address whether CIF-1 functionally interacts with the CSN, we inactivated *cif-1* by injecting *cif-1* dsRNA into young adults and examined the first embryonic divisions using DIC time-lapse microscopy. Most injected animals were sterile and ceased to produce embryos. Fortunately, we were able to record several *cif-1*(*RNAi*) embryos ($n = 10$), most likely those in which *cif-1* was only partially depleted. Interestingly, two of these embryos displayed severe defects in MEI-1-dependent microtubule remodeling, analogous to the defects that arise upon inactivation

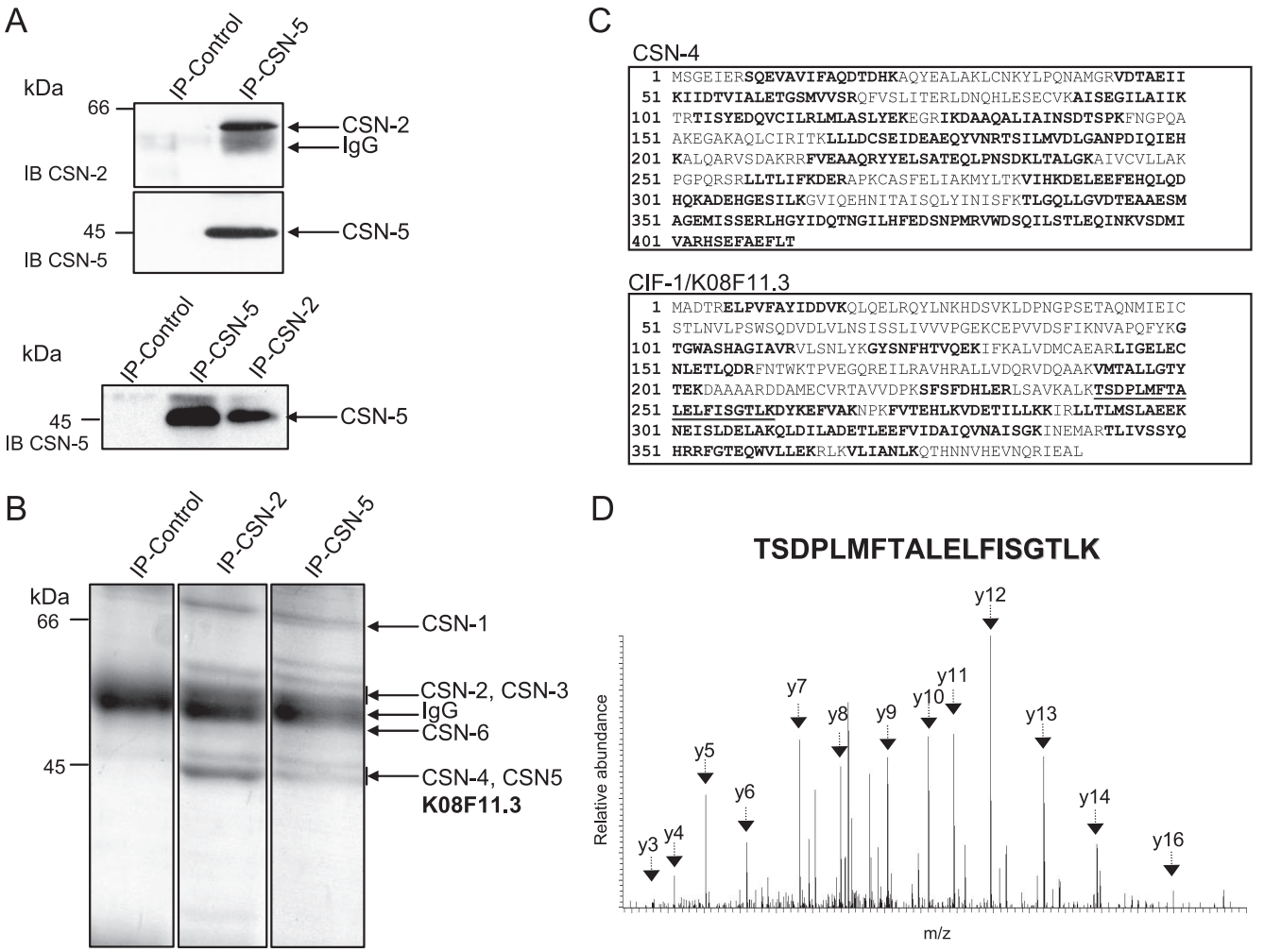


FIG. 2. Proteomic analysis of the CSN in *C. elegans* embryos by tandem mass spectrometry (LC-MS/MS). (A) Mock (IP-Control), CSN-5 (IP-CSN-5), and CSN-2 (IP-CSN-2) immunopurifications were analyzed by immunoblotting (IB) using specific CSN-2 and CSN-5 antibodies. (B) The CSN complex was affinity purified from 30 mg of embryonic extracts using 50 μg of anti-CSN-5 and anti-CSN-2 antibodies. Bound proteins were eluted, separated by SDS-PAGE, and stained with Coomassie colloidal blue. A mock purification was performed with IgG purified from preimmune serum (IP-Control). The arrows indicate the positions of the CSN subunits identified by LC-MS/MS. (C) Amino acid sequence of CSN-4 and CIF-1. The amino acid sequences of the peptides identified by MS/MS in CSN-5 immunoprecipitates are in boldface. (D) The MS/MS spectrum of the CIF-1 peptide TSDPLMFTALELFISGTLK, which is underlined in panel C, is presented. The arrows indicate the positions of y-type ions.

of other CSN subunits (31, 44). Whereas in wild-type embryos the mitotic spindle assembled and elongated along the long anterior-posterior axis after 90° rotation of the nucleocentrosomal complex, it was not correctly oriented and elongated transversally to this axis in these *cif-1*(*RNAi*) embryos (Fig. 4A, d). Moreover, the nuclei were incorrectly positioned too close to the cell cortex during interphase of two-cell stage embryos (Fig. 4A, e). Finally, cytokinesis often failed, leading to the formation of multinucleated cells with tetrapolar spindles (Fig. 4A, f). These observations suggest that CIF-1, like the other CSN subunits, controls MEI-1 degradation through CUL-3 deneddylation. Indeed, partial inactivation of *cif-1* led to a significant accumulation of neddylated CUL-3 (Fig. 4B), accompanied by increased levels of MEI-1 (Fig. 4C and D). Taken together, these results strongly suggest that CIF-1 is a novel and functionally important CSN subunit that is required for CUL-3 deneddylation and concomitant MEI-1 degradation in early embryos.

**CIF-1 is an evolutionarily conserved eIF3m subunit related to Csn7 family members.** Sequence comparisons revealed that CIF-1 is distantly related to the Csn7 family (Fig. 5). Moreover, CIF-1 contains a C-terminal PCI domain (amino acids 279 to 369), which is also present in Csn1, -2, -3, -4, -7, and -8. Multiple sequence alignments between CIF-1 and Csn7 from *H. sapiens* and *D. melanogaster* revealed significant sequence similarities within and immediately upstream of the PCI domain, but not outside this region (Fig. 5A). In addition, CIF-1 is much larger than all other Csn7 family members, which display significant sequence identity with each other over their entire lengths. As mentioned, PCI domains are also found in subunits of the proteasome lid subcomplex and the eukaryotic translation initiation factor eIF3 (23). Surprisingly, given its

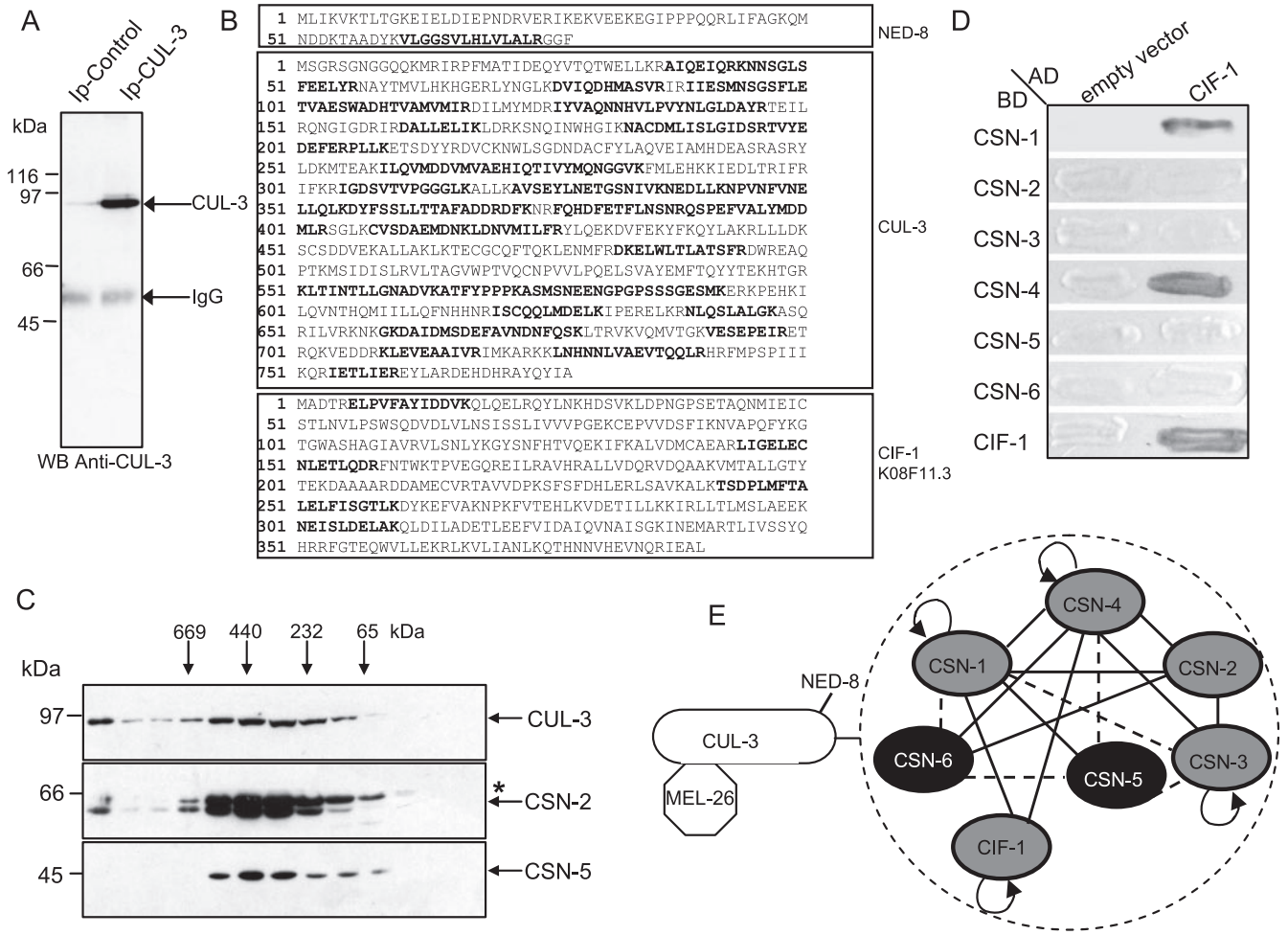


FIG. 3. K08F11.3/CIF-1 interacts physically with the CSN. (A) CUL-3 was immunopurified from embryonic extracts (10 mg) using affinity-purified anti-CUL-3 antibodies (Ip-CUL-3). A control immunopurification was performed with IgG purified from preimmune serum (Ip-Control). A fraction (1/20) of the immunoprecipitates was analyzed by immunoblotting (WB) using CUL-3 antibodies. The remaining fractions of the immunoprecipitates were separated by SDS-PAGE and analyzed by tandem mass spectrometry sequencing (LC-MS/MS). (B) Amino acid sequences of NED-8, CUL-3, and CIF-1. The amino acid sequences of the peptides identified by MS/MS in CUL-3 immunoprecipitates are in boldface. (C) Embryonic extracts were fractionated by size exclusion chromatography on a Superose 6 column (24 ml), and 1-ml fractions (fractions 9 to 21, from left to right) were collected and analyzed by immunoblotting using CSN-2-, CSN-5-, and CUL-3-specific antibodies. The asterisk marks a nonspecific band recognized by the anti-CSN-2 antibody. (D) CIF-1 binds CSN-1 and CSN-4 in yeast two-hybrid experiments. Yeast cells expressing CIF-1 and the indicated CSN subunits fused to the Gal4 DNA binding domain (BD) were mated with cells expressing CIF-1 fused to the activation domain (AD). Expression of the β-galactosidase reporter was analyzed by filter assay. (E) Schematic representation of the interaction network identified by yeast two-hybrid experiments and LC-MS/MS analysis. The gray circles mark subunits with a PCI domain, while the black circles represent subunits with an MPN domain.

evident functional role in the CSN, CIF-1 displays extensive sequence similarity over its entire length with several GA17/eIF3m-related proteins from different species, including GA17 (*H. sapiens*) and SPAC1751.03 (*S. pombe*), as well as the product of the gene annotated CG8309 (*D. melanogaster*) (Fig. 5B and C).

Several lines of evidence suggest that GA17 family members are components of the eIF3 complex. First, GA17 has been recovered in eIF3 purifications from HeLa cells and rabbit reticulocytes (56). Second, the *S. pombe* homologue, recently named eIF3m, is essential for protein translation (68). Since the *C. elegans* genome lacks a bone fide Csn7 subunit and contains only *cif-1* (Fig. 5C), we considered the possibility that CIF-1 might be part of the functionally distinct but evolutionarily related eIF3 and CSN complexes. Indeed, CIF-1 specifically interacted with the MPN subunit eIF-3.F by yeast two-hybrid analysis, suggesting that CIF-1 might also be an integral component of the eIF3 complex in *C. elegans* (see Fig. 7A). To corroborate these data, we inactivated *cif-1* by RNAi in L1 larvae and compared the resulting phenotypes to those observed after inactivation of *eif-3.a* and *eif-3.b*, two core subunits of the eIF3 complex. Interestingly, we found that *cif-1*(*RNAi*), *eif-3.a*(*RNAi*), and *eif-3.b*(*RNAi*) animals arrested at the same larval stage (Fig. 6A). A similar arrest was observed upon growth of L1 larvae on NGM plates containing 50 μg/ml of the translation inhibitor CHX (data not shown). In contrast, *csn-2*(*ok1288*), *csn-5*(*ok1064*), and *csn-6*(*ok1604*) null mutant animals were able to progress through the adult stage, although

TABLE 2. LC-MS/MS analysis of immunopurified CSN-2, CSN-5, and CUL-3 protein complexes from *C. elegans* embryos

| Bait | Protein | Coverage (%) | Mass (Da) |
|---|---|---|---|
| CSN-2 | CSN-1 | 36 | 68,930 |
| | CSN-2 | 37 | 56,973 |
| | CSN-3 | 23 | 56,305 |
| | CSN-4 | 64 | 46,503 |
| | CSN-5 | 50 | 41,267 |
| | CSN-6 | 36 | 47,611 |
| | CIF-1 | 37 | 44,341 |
| CSN-5 | CUL-3 | 13 | 90,691 |
| | CSN-1 | 38 | 68,930 |
| | CSN-2 | 45 | 56,973 |
| | CSN-3 | 26 | 56,305 |
| | CSN-4 | 64 | 46,503 |
| | CSN-5 | 60 | 41,267 |
| | CSN-6 | 23 | 47,611 |
| | CIF-1 | 48 | 44,341 |
| CUL-3 | CUL-3 | 50 | 90,691 |
| | MEL-26 | 3 | 44,920 |
| | NED-8 | 18 | 8,624 |
| | CIF-1 | 14 | 44,341 |
| | CSN-1 | 3 | 68,930 |
| | CSN-5 | 5 | 41,267 |

they were sterile and accumulated neddylated forms of CUL-3 as expected (Fig. 6B, C, D, and E). Moreover, CSN-2 and CSN-5 protein levels were dramatically reduced in *csn-6*(*ok1604*) homozygous null mutant animals (Fig. 6E). These results clearly indicate that, in contrast to *cif-1*, the CSN complex is not required for progression through the larval stages. In contrast to inactivation of CSN subunits, we observed that RNAi inactivation of *cif-1* or *eif-3.a* in L4 larvae resulted in a highly penetrant maternal sterile phenotype, with the brood size being reduced by 50 to 90% in these animals. These observations suggest that CIF-1 also fulfils a CSN-independent function, most likely in translation initiation within the eIF3 complex. Indeed, *cif-1*(*RNAi*) animals, like *eif-3.a*(*RNAi*) animals, were three to five times more sensitive than wild-type animals to low doses of the translational inhibitor CHX (Fig. 7B). To directly measure translation efficiency, we compared incorporation of [$^{35}$S] methionine into proteins in *cif-1*(*RNAi*), *eif-3.a*(*RNAi*), and wild-type larvae (Fig. 7C and D). Importantly, [$^{35}$S]methionine incorporation was reduced to 56% in *cif-1*(*RNAi*) larvae compared to the wild type. For comparison, incorporation dropped to 37% in *eif-3a*(*RNAi*) larvae treated similarly (Fig. 7C and D). Taken together, these observations

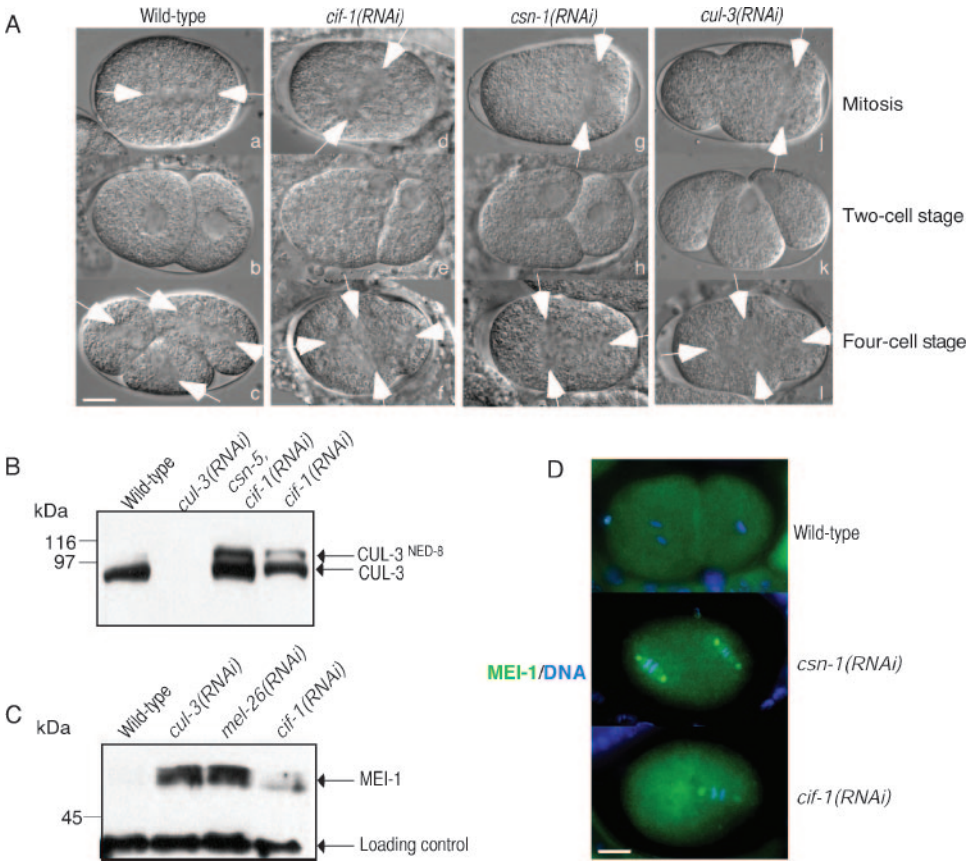


FIG. 4. CIF-1 controls CUL-3 deneddylation and MEI-1 degradation in *C. elegans* embryos. (A) The first two divisions of (a to c) wild-type, (d to f) *cif-1*(*RNAi*), (g to i) *csn-1*(*RNAi*), and (j to l) *cul-3*(*RNAi*) embryos were analyzed by DIC microscopy. The embryos are oriented along their anterior-posterior axes from left to right. The mitotic spindle (marked by white arrows) was not correctly oriented and aligned perpendicularly to the anterior-posterior axis in *cif-1*(*RNAi*), *csn-1*(*RNAi*), and *cul-3*(*RNAi*) embryos (compare d, g, and j to a). (B) Extracts were prepared from wild-type, *cul-3*(*RNAi*), *cif-1*(*RNAi*), and *csn-5*(*RNA*i); *cif-1*(*RNAi*) embryos and examined by immunoblotting them with CUL-3-specific antibodies. (C) Extracts prepared from wild-type, *cul-3*(*RNAi*), *mel-26*(*RNAi*), and *cif-1*(*RNAi*) embryos were analyzed by immunoblotting them with anti-MEI-1 antibodies. (D) Micrographs of MEI-1 (green) and DNA (blue) stainings of fixed wild-type, *csn-1*(*RNAi*), and *cif-1*(*RNAi*) embryos in mitosis. The scale bar represents 10 μm.

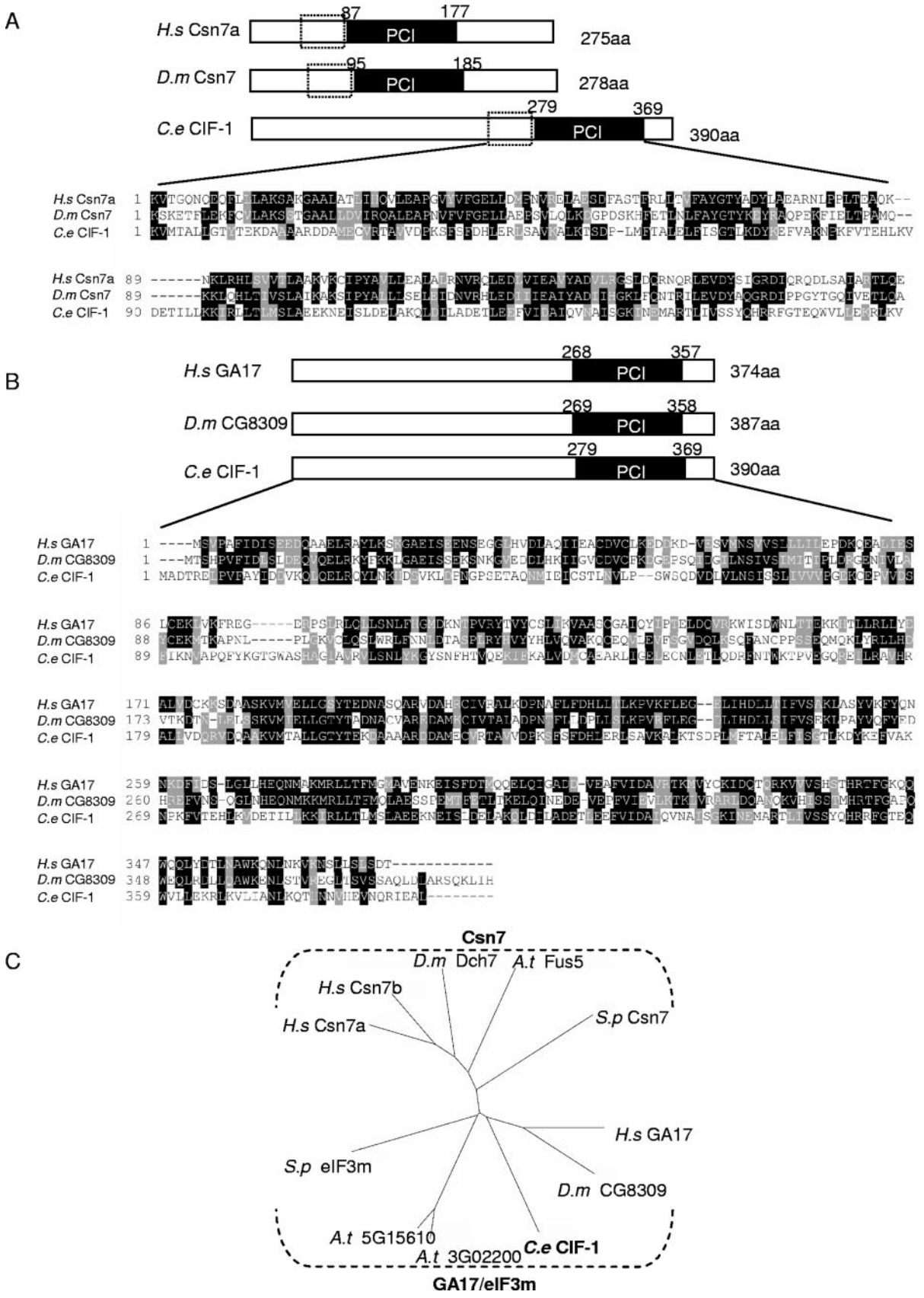


FIG. 5. CIF-1 is an evolutionarily conserved eIF3m-like subunit related to Csn7. (A) The domain organizations of CIF-1 and Csn7 family members (*H. sapiens* [*H.s*] Csn7a and *D. melanogaster* [*D.m*] Dch7) are compared. Similarities span the PCI domain and the region immediately

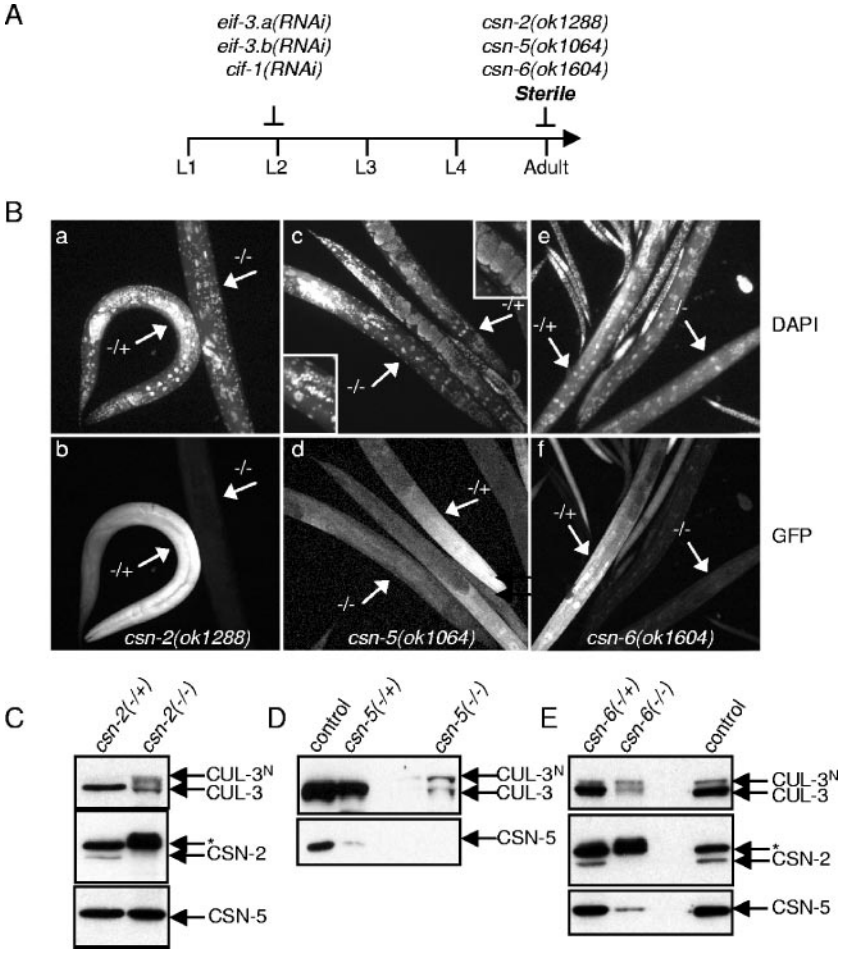


FIG. 6. CIF-1 fulfils a CSN-independent function. (A) After hatching, wild-type *C. elegans* progresses through four larval stages (L1 to L4) before reaching adulthood. The scheme shows a comparison of the larval development of wild-type and homozygous *csn-2*(*ok1288*), *csn-5*(*ok1064*), and *csn-6*(*ok1604*) worms and animals fed on bacteria expressing dsRNA to deplete *cif-1*, *eif-3.a*, or *eif-3.b*. Note that *csn* mutant animals progress to the adult stage, while *cif-1*(*RNAi*), *eif-3.a*(*RNAi*), and *eif-3.b*(*RNAi*) animals arrest as larvae. (B) Heterozygous and homozygous *csn-2*(*ok1288*) (a and b), *csn-5*(*ok1064*) (c and d), and *csn-6*(*ok1604*) (e and f) animals were stained with DAPI and visualized by fluorescence microscopy. Note that the homozygous (GFP-negative) worms progressed to adulthood but were sterile, because of the absence of a germ line, as visualized by DAPI staining. (C) Protein extracts were prepared from heterozygous *csn-2*(*ok1288*)/+ and homozygous *csn-2*(*ok1288*) animals, and immunoblotted with CUL-3-, CSN-2-, and CSN-5-specific antibodies. (D) Protein extracts were prepared from wild-type, heterozygous *csn-5*(*ok1064*)/+, and homozygous *csn-5*(*ok1064*) animals and immunoblotted with CUL-3- and CSN-5-specific antibodies. (E) Protein extracts were prepared from heterozygous *csn-6*(*ok1604*)/+ and homozygous *csn-6*(*ok1604*) animals and a wild-type control and immunoblotted with CUL-3-, CSN-2-, and CSN-5-specific antibodies.

indicate that CIF-1 is an essential subunit of the eIF3 complex required for protein translation in *C. elegans* (Fig. 8D).

**GA17 and Csn7a are dedicated subunits of the eIF3 and the CSN complexes in mammalian cells.** To determine whether the dual role of CIF-1 was conserved through evolution, we tested whether human GA17 and Csn7a might exclusively associate with the eIF3 and CSN complexes, respectively, or whether they might be shared subunits of both complexes. To this end, we established stable cell lines expressing human Csn7a, GA17, and eIF3e fused to three repeats of the FLAG epitope [$(FLAG)_3$] and immunopurified protein complexes using anti-FLAG agarose beads (Fig. 8A and B). As a control, we performed mock purifications from HEK 293T cells harboring an empty vector. Protein complexes were eluted and analyzed by LC-MS/MS after direct digestion of captured proteins without gel separation (see Materials and Methods). We identified

upstream. The positions of the PCI domains were defined by SMART. A multiple alignment of the PCI domains and the residues located upstream from Csn7 family members (*H. sapiens* and *D. melanogaster*) CIF-1 is presented. (B) The CIF-1 protein sequence was aligned with human GA17 and *D. melanogaster* CG8309 using ClustalW. The alignment was shaded with BOXSHADE. (C) A phylogenetic analysis of Csn7 and GA17/eIF3m family members is represented. Csn7 protein sequences from human (Csn7a/Csn7b), *D. melanogaster*, *A. thaliana* (Fus5) (*A. t*), and *S. pombe* Csn7 (*S. p*) are shown in the upper part (CSN), while GA17/eIF3m protein sequences are presented in the lower part (eIF3).

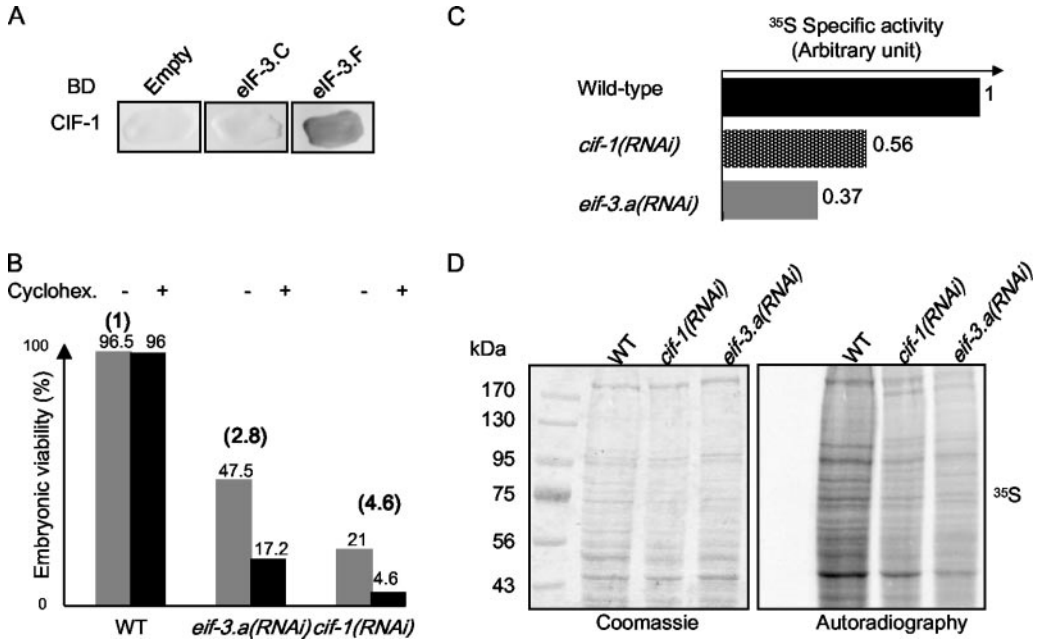


FIG. 7. CIF-1 interacts with eIF-3.F and is required for protein translation. (A) CIF-1 binds eIF-3.F in yeast two-hybrid experiments. Yeast cells were cotransformed with plasmids expressing CIF-1 fused to the GAL4 binding domain (BD) and eIF-3.C or eIF-3.F fused to the GAL4 DNA activation domain. Expression of the β-galactosidase reporter was analyzed by filter assay. (B) Low doses of CHX exacerbate the lethality induced by depletion of *eif-3.a* and *cif-1* (2.8- and 4.6-fold, respectively). L4 animals were fed at 16°C on control bacteria (wild type [WT]) or bacteria expressing dsRNA to deplete *eif-3.a* and *cif-1* in the presence (+) or absence (−) of low doses of CHX (5 μg/ml). After 30 h, five animals from each plate were transferred to regular OP50 plates, where they laid eggs for 7 h. Embryonic viability was then determined and plotted as a percentage of total embryos. (C) Wild-type, *cif-1*(*RNAi*), and *eif-3.a*(*RNAi*) larvae were incubated with bacteria prelabeled with [$^{35}$S]methionine. After a chase of 1 hour with cold bacteria, worm lysates were prepared, and their specific activities were determined and plotted. The value obtained for wild-type lysate was arbitrarily defined as 1. (D) Radiolabeled worm lysates (20 μg) were separated on SDS-PAGE, which was stained with Coomassie brilliant blue and exposed for autoradiography.

apparent stoichiometric amounts of all subunits of the human eIF3 complex in association with GA17, including the subunits eIF3a, -b, -c, -d, -e, -f, -g, -h, -i, -j, -k, and -l (Fig. 8C and Table 3). GA17 and the other eIF3 subunits were also identified in eIF3e immunopurifications (Table 3). In contrast, not a single CSN subunit copurified with GA17 or eIF3e under these conditions. Conversely, neither GA17 nor any eIF3 subunits were recovered in the $(FLAG)_3$-Csn7a immunopurification, despite identification of Csn1, -2, -3, -4, -5, -6, and -8. Immunoblot analysis with polyclonal antibodies raised against multiple eIF3 subunits confirmed that GA17 specifically associated with eIF3, but not CSN subunits (Fig. 8A). These results indicate that in human cells, and likely in all species that contain a bona fide Csn7 subunit, GA17 is an exclusive member of the eIF3 complex, while Csn7 is dedicated to the CSN complex (Fig. 8C).

## DISCUSSION

**The CSN sustains MEL-26 protein levels by counteracting its autocatalytic instability in *C. elegans*.** We have shown that the CSN complex physically interacts with the CUL-3-based ligase and counteracts the autocatalytic instability of the BTB adaptor MEL-26. While MEI-1 and neddylated forms of CUL-3 strongly accumulated upon inactivation of the CSN complex, MEL-26 protein levels were dramatically reduced (Fig. 1B and C). Since CUL-3 neddylation is essential for MEL-26 degradation (38), these observations indicate that a balance between neddylation and deneddylation is needed to maintain sufficient MEL-26 protein levels required for MEI-1 degradation. Neddylation may trigger MEL-26 autoubiquitination by stimulating the recruitment of the ubiquitin-conjugated E2. To test this hypothesis, we assessed the efficiency of MEL-26 autoubiquitination using Cul3-Rbx1 complex neddylated in vitro. While Cul3 was readily neddylated, MEL-26 autoubiquitination was not significantly stimulated under these experimental conditions (data not shown). Alternatively, neddylation may trigger MEL-26 autoubiquitination by promoting its assembly into the Cul3 complex through dissociation of the CAND-1 inhibitor (37, 66). However, *cand-1* inactivation does not give rise to embryonic lethality (51), and we were unable to detect peptides corresponding to CAND-1 in the LC-MS/MS analysis of immunopurified CUL-3 complexes. While this result might be explained if CAND-1 and CUL-3 antibodies compete for the same binding site, there is currently no experimental evidence to support a role of CAND-1 in the regulation of the CUL-3–MEL-26 complex. Clearly, further work will be required to address the precise role of CUL-3 neddylation in MEL-26 degradation.

The total number of CRL substrate-specific adaptors is estimated at more than 500 proteins (42). Are all these adaptors unstable? Indeed, many adaptors of all CRL subfamilies have been shown to be actively degraded by the ubiquitin-proteasome system in all species, including the F-box proteins

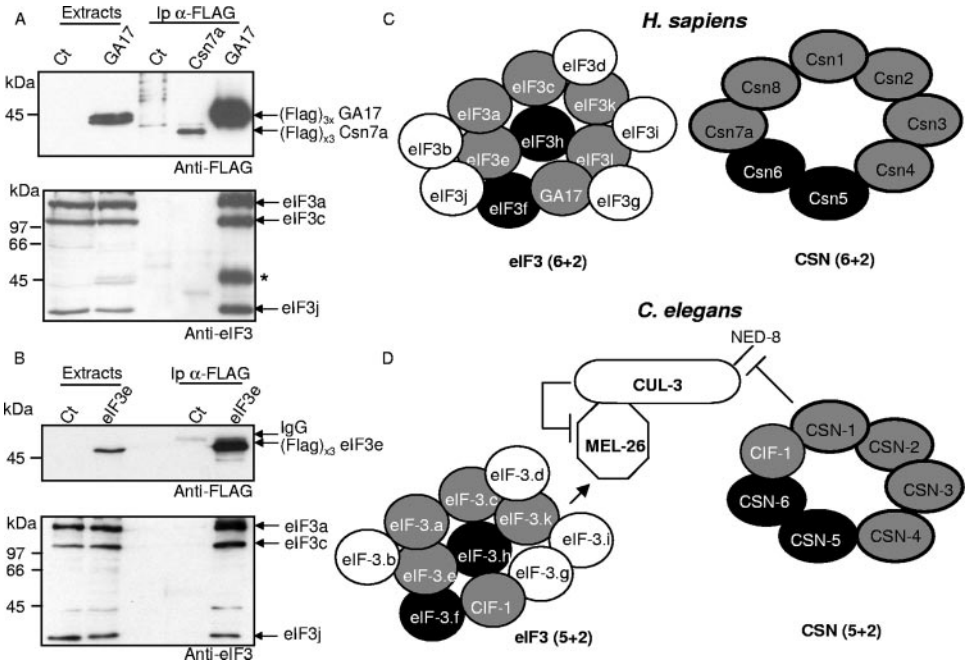


FIG. 8. In contrast to *C. elegans*, the human genome encodes dedicated subunits of the eIF3 and CSN complexes termed Csn7a/b and GA17. (A) Extracts of HEK 293T cells stably expressing $(FLAG)_3$-GA17, $(FLAG)_3$-Csn7a, or an empty vector (Ct) were incubated with immobilized anti-FLAG antibodies. Total extracts or a fraction (one-fifth) of the immunoprecipitates (Ip) were analyzed by immunoblotting them with specific FLAG (top) or eIF3 (bottom) antibodies. The asterisk marks signal remaining from the anti-FLAG Western blot. (B) Extracts of HEK 293T cells stably expressing $(FLAG)_3$-eIF3e or an empty vector (Ct) were incubated with immobilized anti-FLAG antibodies. Total extracts or a fraction (one-fifth) of the immunoprecipitates were analyzed by immunoblotting them with specific FLAG (top) or eIF3 (bottom) antibodies. (C) Schematic representation of the interaction network defined by LC-MS/MS experiments after immunopurification of $(FLAG)_3$-Csn7a and $(FLAG)_3$-GA17 from HEK 293T cells. The open and gray circles represent subunits with a PCI domain, and the black circles represent subunits with an MPN domain. (D) CIF-1 is shared between the CSN and the eIF3 complex in *C. elegans*. Since the assembly of CIF-1 into the CSN and eIF3 complexes likely requires the PCI domain, the association of CIF-1 with these complexes is expected to be mutually exclusive. In *C. elegans*, the eIF3 complex and the CSN may cooperate to sustain MEL-26 protein levels.

FWD-1 (*Neurospora crassa*), Pop1 (*S. pombe*), and Skp2 (*H. sapiens*); the BTB proteins Btb3 (*S. pombe*) and MEL-26 (*C. elegans*); and the Decaf proteins Cdt2 in *S. pombe* and Ddb2 in mammalian cells.

Many unstable CRL adaptors are degraded by an autocatalytic mechanism. Interestingly, the CSN was shown to counteract the autocatalytic instability of FWD-1 (19), Skp2 (12), Fbx4 (10), and Pop1 (58), and in at least some cases, this inhibitory effect of the CSN may be regulated by extracellular signals. For example, the *D*NA *d*amage *b*inding protein 2 (DDB2) stably associates with Cul4A under normal conditions but is rapidly degraded upon UV damage after neddylation of CUL4 (17, 54). These observations raise the attractive possibility that many adaptors may be stably assembled into CSN-bound cullin complexes but become unstable upon activation of the CRL in response to specific cues.

However, CSN-regulated autocatalytic instability is not the only mechanism controlling adaptor stability. Indeed, ubiquitin-dependent degradation of the Decaf protein Cdt2 in *S. pombe* is not controlled by an autocatalytic mechanism, indicating that other factors regulate Cdt2 protein levels (36). Like the adaptors Skp2 and Tome-1, which play critical roles in cell cycle progression (5, 61), Cdt2 degradation might be at least in part controlled by the APC/C. Further work will be required to identify the different molecular mechanisms controlling Cdt2 instability.

Finally, we note that in addition to the substrate-specific adaptors, other CRL subunits also become unstable when the CSN is inactivated, including Cul1 and Cul3 in *D. melanogaster* (63), Rbx1 in human cells (22), and Cul1 and Skp1 in *N. crassa* (19). Although MEL-26 was much more severely affected, we also observed a significant reduction of CUL-3 levels in *csn* homozygous null animals and in *csn-1*(*RNAi*) embryos (Fig. 1B and 6C, D, and E), indicating that the CSN regulates the level of core CRL subunits in *C. elegans*.

**The CSN counteracts MEL-26 instability, most likely through CUL-3 deneddylation.** In *S. pombe*, Ubp12 binds to CRL complexes and is thought to catalyze the deubiquitination of CRL adaptors in conjunction with the CSN (58, 69). However, while we were able to readily immunopurify the entire CSN complex and associated CUL-3 components, we did not detect a bound Ubp12-like protein. Likewise, Ubp12 is apparently not associated with the purified *N. crassa* CSN complex, nor does deletion of Ubp12 cause a detectable phenotype in this organism (19). In mammalian cells, a catalytically inactive version of Csn5, which does not prevent Ubp12 recruitment to the CSN complex, still causes depletion of F-box proteins (10). Together, these observations thus suggest that in most instances, not Ubp12 but CSN-dependent deneddylation of cullins might be the main enzymatic activity that controls CRL adaptor protein levels.

TABLE 3. Biochemical identification of human GA17, eIF3e, and Csn7a protein complexes by LC-MS/MS analysis

| Bait | Protein | Coverage (%) | Mass (Da) |
|---|---|---|---|
| GA17 | eIF3a | 58 | 166,867 |
| | eIF3b | 60 | 92,833 |
| | eIF3c | 42 | 105,960 |
| | eIF3d | 69 | 64,560 |
| | eIF3e | 67 | 52,587 |
| | eIF3f | 55 | 37,654 |
| | eIF3g | 68 | 35,959 |
| | eIF3h | 75 | 40,076 |
| | eIF3i | 82 | 36,878 |
| | eIF3j | 20 | 29,087 |
| | eIF3k | 68 | 25,329 |
| | eIF3l | 53 | 66,912 |
| | eIF3m/GA17 | 63 | 42,900 |
| eIF3e | eIF3a | 28 | 166,867 |
| | eIF3b | 38 | 92,833 |
| | eIF3c | 26 | 105,960 |
| | eIF3d | 48 | 64,560 |
| | eIF3e | 50 | 52,587 |
| | eIF3f | 34 | 37,654 |
| | eIF3g | 34 | 35,959 |
| | eIF3h | 18 | 40,076 |
| | eIF3i | 40 | 36,878 |
| | eIF3j | 16 | 29,087 |
| | eIF3k | 42 | 25,329 |
| | eIF3l | 27 | 66,912 |
| | eIF3m/GA17 | 24 | 42,900 |
| Csn7a | Csn1 | 45 | 57,072 |
| | Csn2 | 56 | 51,819 |
| | Csn3 | 44 | 46,267 |
| | Csn4 | 75 | 46,454 |
| | Csn5 | 53 | 37,764 |
| | Csn6 | 50 | 33,896 |
| | Csn7a | 62 | 30,438 |
| | Csn8 | 61 | 23,268 |

**The *C. elegans* CSN complex contains seven subunits, including the novel subunit CIF-1.** We identified CIF-1 as a novel PCI domain-containing subunit of the CSN complex. CIF-1 was recovered in apparent stoichiometric amounts with all known CSN subunits in CSN-2 and CSN-5 immunoprecipitates (Fig. 2). Consistent with these observations, CIF-1 also copurified with CUL-3, together with MEL-26, NED-8, CSN-1, and CSN-5 (Fig. 3). As for other CSN subunits, *cif-1* inactivation resulted in partial accumulation of MEI-1 and neddylated forms of CUL-3 in embryos (Fig. 4). A partial accumulation was expected in this specific case, since the embryos analyzed in these experiments were laid by animals in which *cif-1* was only partially depleted. Indeed, our results indicate that CIF-1 is shared between the CSN and the eIF3 complex, the latter being essential for larval development (Fig. 6A and 8D) (see below).

The sequence similarity between CIF-1 and Csn7 members, which spans the PCI domain and the region immediately upstream of it, strongly suggests that CIF-1 functions as the bone fide Csn7 subunit in *C. elegans*. In support of this notion, CIF-1, like Csn7 in mammals, plants, and flies (60), appears to interact directly with CSN-4 and also binds CSN-1 (Fig. 3D). Notably, an interaction between CIF-1 and CSN-4 has also been detected in a large-scale two-hybrid screen (34).

**CIF-1 links protein translation and degradation machineries.** In addition to its role in the CSN complex, our data indicate that CIF-1 is also an integral component of the eIF3 complex in both worm and human cells. This interaction is functionally relevant because *cif-1* inactivation results in a developmental-arrest phenotype similar to that observed upon inactivation of eIF3 core subunits, but not in *csn-2*(*ok1288*), *csn-5*(*ok1064*), or *csn-6*(*1604*) null mutant animals (Fig. 6). Moreover, we found that [$^{35}$S]methionine incorporation was significantly reduced in *cif-1*(*RNAi*) larvae, suggesting that *cif-1* depletion causes developmental arrest by impairing translation (Fig. 7). In support of this hypothesis, partial depletion of *cif-1* confers sensitivity to low doses of the translation inhibitor CHX (Fig. 7B). Finally, CIF-1 binds eIF-3.F in yeast two-hybrid experiments (Fig. 7A), and we have identified the human CIF-1 homologue GA17 as a core subunit of the eIF3 complex. Indeed, LC-MS/MS analysis of immunopurified $(FLAG)_3$-GA17 unambiguously identified all 12 subunits of the eIF3 complex, and conversely, GA17 was also identified in $(FLAG)_3$-eIF3e pull-downs (Fig. 8A and B and Table 3), together with all other subunits of the eIF3 complex. Thus, like the CSN and the proteasome lid, the eIF3 complex also contains six PCI- and two MPN-based subunits (Fig. 8C).

Our results identify CIF-1 as a shared subunit between the CSN and the eIF3 complexes. This dual role of CIF-1 suggests the intriguing possibility that the CSN and the translation machinery cooperate to sustain the levels of MEL-26 and probably other proteins (Fig. 8D). In support of this prediction, *N. crassa csn2* mutants are highly sensitive to the translational inhibitor CHX, indicating that in this system the CSN and the protein translation machinery also cooperate to sustain the levels of the CRL1 adaptor FWD-1 (19).

Analogous to CIF-1, other PCI domain proteins in several lower organisms may also exhibit dual functions. For example, in budding yeast, the proteasomal lid protein Rpn5 copurifies with several CSN subunits and may function in these two different PCI-based complexes (14, 15, 29). Likewise, Pci8, which is a CSN subunit distantly related to eIF3e/Int6, interacts with the eIF3 subunit eIF3b/Prt1 on the same binding site as human eIF3e. Since the budding yeast genome does not encode an eIF3e subunit, these results indicate that Pci8 may thus also link the translation and ubiquitin-dependent degradation machineries (50). Finally, in fission yeast, the PCI domain protein eIF3e/int-6 regulates protein translation and proteasome activity via its interaction with Rpn5 (65). Therefore, lower organisms may generally share PCI-based subunits to link protein translation and degradation. In contrast, our results indicate that other mechanisms might operate in mammalian cells, which contain a dedicated set of PCI-containing subunits and thus do not seem to share them among the three complexes. It is possible that the increased complexity in mammalian cells with more than 500 CRL adaptors and, in turn, a plethora of substrates are required to uncouple protein translation and CRL activity. A main challenge for the future will be to shed light on the mechanisms that balance protein translation and degradation in mammalian cells.

## ACKNOWLEDGMENTS

We are grateful to N. Zheng for providing GST-Cul3 and Rbx1 baculoviruses, J. Hershey for the anti-eIF3 antibodies, A. A. Ogunjimi

for six-HIS–Ubc5c, and the International *C. elegans* Gene Knockout Consortium for providing us with the *csn* deletion alleles. Some nematode strains used in this work were provided by the *Caenorhabditis* Genetics Center, which is funded by the NIH National Center for Research Resources (NCRR). We thank P. Weissert and U. Bauer for help with worm cultures in the fermentor and T. Goh, F. A. Yeung, and A.-M. Salter for their help with the analysis of the eIF3E immunopurifications. We also thank L. Zhiqin and D. Dewar for excellent technical assistance.

L.P. was supported by a traveling fellowship from the *Journal of Cell Science* and by an ATIP grant from the Centre National de la Recherche Scientifique (CNRS). S.L.-G. was financed by a fellowship from the Boehringer Ingelheim Funds and the laboratory of M.P. by grants from the SNF and the ETHZ. The laboratory of M.T. was supported by grants from the Canadian Institutes of Health Research and the National Cancer Institute of Canada. M.T. is a Canada Research Chair in Bioinformatics and Functional Genomics.

We declare that we have no conflicting financial interest.

## REFERENCES

1. **Altschul, S. F., T. L. Madden, A. A. Schaffer, J. Zhang, Z. Zhang, W. Miller, and D. J. Lipman.** 1997. Gapped BLAST and PSI-BLAST: a new generation of protein database search programs. Nucleic Acids Res. **25:**3389–3402.
2. **Angers, S., T. Li, X. Yi, M. J. MacCoss, R. T. Moon, and N. Zheng.** 2006. Molecular architecture and assembly of the DDB1-CUL4A ubiquitin ligase machinery. Nature **443:**590–593.
3. **Aravind, L., and C. P. Ponting.** 1998. Homologues of 26S proteasome subunits are regulators of transcription and translation. Protein Sci. **7:**1250–1254.
4. **Asano, K., T. G. Kinzy, W. C. Merrick, and J. W. Hershey.** 1997. Conservation and diversity of eukaryotic translation initiation factor eIF3. J. Biol. Chem. **272:**1101–1109.
5. **Ayad, N. G., S. Rankin, M. Murakami, J. Jebanathirajah, S. Gygi, and M. W. Kirschner.** 2003. Tome-1, a trigger of mitotic entry, is degraded during $G_1$ via the APC. Cell **113:**101–113.
6. **Bowerman, B., and T. Kurz.** 2006. Degrade to create: developmental requirements for ubiquitin-mediated proteolysis during early *C. elegans* embryogenesis. Development **133:**773–784.
7. **Brenner, S.** 1974. The genetics of *Caenorhabditis elegans*. Genetics **77:**71–94.
8. **Chamovitz, D. A., N. Wei, M. T. Osterlund, A. G. von Arnim, J. M. Staub, M. Matsui, and X. W. Deng.** 1996. The COP9 complex, a novel multisubunit nuclear regulator involved in light control of a plant developmental switch. Cell **86:**115–121.
9. **Clark-Maguire, S., and P. E. Mains.** 1994. *mei-1*, a gene required for meiotic spindle formation in *Caenorhabditis elegans*, is a member of a family of ATPases. Genetics **136:**533–546.
10. **Cope, G. A., and R. J. Deshaies.** 2006. Targeted silencing of Jab1/Csn5 in human cells downregulates SCF activity through reduction of F-box protein levels. BMC Biochem. **7:**1.
11. **Cope, G. A., G. S. Suh, L. Aravind, S. E. Schwarz, S. L. Zipursky, E. V. Koonin, and R. J. Deshaies.** 2002. Role of predicted metalloprotease motif of Jab1/Csn5 in cleavage of Nedd8 from Cul1. Science **298:**608–611.
12. **Denti, S., M. E. Fernandez-Sanchez, L. Rogge, and E. Bianchi.** 2006. The COP9 signalosome regulates Skp2 levels and proliferation of human cells. J. Biol. Chem. **281:**32188–32196.
13. **Dow, M. R., and P. E. Mains.** 1998. Genetic and molecular characterization of the *Caenorhabditis elegans* gene, *mel-26*, a postmeiotic negative regulator of mei-1, a meiotic-specific spindle component. Genetics **150:**119–128.
14. **Gavin, A. C., P. Aloy, P. Grandi, R. Krause, M. Boesche, M. Marzioch, C. Rau, L. J. Jensen, S. Bastuck, B. Dumpelfeld, A. Edelmann, M. A. Heurtier, V. Hoffman, C. Hoefert, K. Klein, M. Hudak, A. M. Michon, M. Schelder, M. Schirle, M. Remor, T. Rudi, S. Hooper, A. Bauer, T. Bouwmeester, G. Casari, G. Drewes, G. Neubauer, J. M. Rick, B. Kuster, P. Bork, R. B. Russell, and G. Superti-Furga.** 2006. Proteome survey reveals modularity of the yeast cell machinery. Nature **440:**631–636.
15. **Gavin, A. C., M. Bosche, R. Krause, P. Grandi, M. Marzioch, A. Bauer, J. Schultz, J. M. Rick, A. M. Michon, C. M. Cruciat, M. Remor, C. Hofert, M. Schelder, M. Brajenovic, H. Ruffner, A. Merino, K. Klein, M. Hudak, D. Dickson, T. Rudi, V. Gnau, A. Bauch, S. Bastuck, B. Huhse, C. Leutwein, M. A. Heurtier, R. R. Copley, A. Edelmann, E. Querfurth, V. Rybin, G. Drewes, M. Raida, T. Bouwmeester, P. Bork, B. Seraphin, B. Kuster, G. Neubauer, and G. Superti-Furga.** 2002. Functional organization of the yeast proteome by systematic analysis of protein complexes. Nature **415:**141–147.
16. **Glickman, M. H., D. M. Rubin, O. Coux, I. Wefes, G. Pfeifer, Z. Cjeka, W. Baumeister, V. A. Fried, and D. Finley.** 1998. A subcomplex of the proteasome regulatory particle required for ubiquitin-conjugate degradation and related to the COP9-signalosome and eIF3. Cell **94:**615–623.
17. **Groisman, R., J. Polanowska, I. Kuraoka, J. Sawada, M. Saijo, R. Drapkin, A. F. Kisselev, K. Tanaka, and Y. Nakatani.** 2003. The ubiquitin ligase activity in the DDB2 and CSA complexes is differentially regulated by the COP9 signalosome in response to DNA damage. Cell **113:**357–367.
18. **Guthrie, C., and G. R. Fink.** 1991. Guide to yeast genetics and molecular biology. Methods Enzymol. **194:**1–863.
19. **He, Q., P. Cheng, and Y. Liu.** 2005. The COP9 signalosome regulates the *Neurospora* circadian clock by controlling the stability of the SCFFWD-1 complex. Genes Dev. **19:**1518–1531.
20. **Hershko, A., and A. Ciechanover.** 1998. The ubiquitin system. Annu. Rev. Biochem. **67:**425–479.
21. **Hershko, A., H. Heller, S. Elias, and A. Ciechanover.** 1983. Components of ubiquitin-protein ligase system. Resolution, affinity purification, and role in protein breakdown. J. Biol. Chem. **258:**8206–8214.
22. **Hetfeld, B. K., A. Helfrich, B. Kapelari, H. Scheel, K. Hofmann, A. Guterman, M. Glickman, R. Schade, P. M. Kloetzel, and W. Dubiel.** 2005. The zinc finger of the CSN-associated deubiquitinating enzyme USP15 is essential to rescue the E3 ligase Rbx1. Curr. Biol. **15:**1217–1221.
23. **Hofmann, K., and P. Bucher.** 1998. The PCI domain: a common theme in three multiprotein complexes. Trends Biochem. Sci. **23:**204–205.
24. **Hori, T., F. Osaka, T. Chiba, C. Miyamoto, K. Okabayashi, N. Shimbara, S. Kato, and K. Tanaka.** 1999. Covalent modification of all members of human cullin family proteins by NEDD8. Oncogene **18:**6829–6834.
25. **Jin, J., E. E. Arias, J. Chen, J. W. Harper, and J. C. Walter.** 2006. A family of diverse Cul4-Ddb1-interacting proteins includes Cdt2, which is required for S phase destruction of the replication factor Cdt1. Mol. Cell **23:**709–721.
26. **Kapelari, B., D. Bech-Otschir, R. Hegerl, R. Schade, R. Dumdey, and W. Dubiel.** 2000. Electron microscopy and subunit-subunit interaction studies reveal a first architecture of COP9 signalosome. J. Mol. Biol. **300:**1169–1178.
27. **Kawakami, T., T. Chiba, T. Suzuki, K. Iwai, K. Yamanaka, N. Minato, H. Suzuki, N. Shimbara, Y. Hidaka, F. Osaka, M. Omata, and K. Tanaka.** 2001. NEDD8 recruits E2-ubiquitin to SCF E3 ligase. EMBO J. **20:**4003–4012.
28. **Kipreos, E. T., L. E. Lander, J. P. Wing, W. W. He, and E. M. Hedgecock.** 1996. *cul-1* is required for cell cycle exit in *C. elegans* and identifies a novel gene family. Cell **85:**829–839.
29. **Krogan, N. J., G. Cagney, H. Yu, G. Zhong, X. Guo, A. Ignatchenko, J. Li, S. Pu, N. Datta, A. P. Tikuisis, T. Punna, J. M. Peregrin-Alvarez, M. Shales, X. Zhang, M. Davey, M. D. Robinson, A. Paccanaro, J. E. Bray, A. Sheung, B. Beattie, D. P. Richards, V. Canadien, A. Lalev, F. Mena, P. Wong, A. Starostine, M. M. Canete, J. Vlasblom, S. Wu, C. Orsi, S. R. Collins, S. Chandran, R. Haw, J. J. Rilstone, K. Gandi, N. J. Thompson, G. Musso, P. St Onge, S. Ghanny, M. H. Lam, G. Butland, A. M. Altaf-Ul, S. Kanaya, A. Shilatifard, E. O'Shea, J. S. Weissman, C. J. Ingles, T. R. Hughes, J. Parkinson, M. Gerstein, S. J. Wodak, A. Emili, and J. F. Greenblatt.** 2006. Global landscape of protein complexes in the yeast *Saccharomyces cerevisiae*. Nature **440:**637–643.
30. **Kurz, T., N. Ozlu, F. Rudolf, S. M. O'Rourke, B. Luke, K. Hofmann, A. A. Hyman, B. Bowerman, and M. Peter.** 2005. The conserved protein DCN-1/Dcn1p is required for cullin neddylation in *C. elegans* and *S. cerevisiae*. Nature **435:**1257–1261.
31. **Kurz, T., L. Pintard, J. H. Willis, D. R. Hamill, P. Gonczy, M. Peter, and B. Bowerman.** 2002. Cytoskeletal regulation by the Nedd8 ubiquitin-like protein modification pathway. Science **295:**1294–1298.
32. **Lammer, D., N. Mathias, J. M. Laplaza, W. Jiang, Y. Liu, J. Callis, M. Goebl, and M. Estelle.** 1998. Modification of yeast Cdc53p by the ubiquitin-related protein Rub1p affects function of the $SCF^{Cdc4}$ complex. Genes Dev. **12:**914–926.
33. **Lewis, J. A., and J. T. Fleming.** 1995. Basic culture methods. Methods Cell Biol. **48:**3–29.
34. **Li, S., C. M. Armstrong, N. Bertin, H. Ge, S. Milstein, M. Boxem, P. O. Vidalain, J. D. Han, A. Chesneau, T. Hao, D. S. Goldberg, N. Li, M. Martinez, J. F. Rual, P. Lamesch, L. Xu, M. Tewari, S. L. Wong, L. V. Zhang, G. F. Berriz, L. Jacotot, P. Vaglio, J. Reboul, T. Hirozane-Kishikawa, Q. Li, H. W. Gabel, A. Elewa, B. Baumgartner, D. J. Rose, H. Yu, S. Bosak, R. Sequerra, A. Fraser, S. E. Mango, W. M. Saxton, S. Strome, S. Van Den Heuvel, F. Piano, J. Vandenhaute, C. Sardet, M. Gerstein, L. Doucette-Stamm, K. C. Gunsalus, J. W. Harper, M. E. Cusick, F. P. Roth, D. E. Hill, and M. Vidal.** 2004. A map of the interactome network of the metazoan *C. elegans*. Science **303:**540–543.
35. **Liakopoulos, D., G. Doenges, K. Matuschewski, and S. Jentsch.** 1998. A novel protein modification pathway related to the ubiquitin system. EMBO J. **17:**2208–2214.
36. **Liu, C., M. Poitelea, A. Watson, S. H. Yoshida, C. Shimoda, C. Holmberg, O. Nielsen, and A. M. Carr.** 2005. Transactivation of *Schizosaccharomyces pombe* cdt2+ stimulates a Pcu4-Ddb1-CSN ubiquitin ligase. EMBO J. **24:**3940–3951.
37. **Liu, J., M. Furukawa, T. Matsumoto, and Y. Xiong.** 2002. NEDD8 modification of CUL1 dissociates $p120^{CAND1}$, an inhibitor of CUL1-SKP1 binding and SCF ligases. Mol. Cell **10:**1511–1518.
38. **Luke-Glaser, S., L. Pintard, C. Lu, P. E. Mains, and M. Peter.** 2005. The BTB protein MEL-26 promotes cytokinesis in *C. elegans* by a CUL-3-independent mechanism. Curr. Biol. **15:**1605–1615.
39. **Lyapina, S., G. Cope, A. Shevchenko, G. Serino, T. Tsuge, C. Zhou, D. A.**

**Wolf, N. Wei, and R. J. Deshaies.** 2001. Promotion of NEDD-CUL1 conjugate cleavage by COP9 signalosome. Science **292:**1382–1385.
40. **Meyer, L. J., S. C. Milburn, and J. W. Hershey.** 1982. Immunochemical characterization of mammalian protein synthesis initiation factors. Biochemistry **21:**4206–4212.
41. **Perkins, D. N., D. J. Pappin, D. M. Creasy, and J. S. Cottrell.** 1999. Probability-based protein identification by searching sequence databases using mass spectrometry data. Electrophoresis **20:**3551–3567.
42. **Petroski, M. D., and R. J. Deshaies.** 2005. Function and regulation of cullin-RING ubiquitin ligases. Nat. Rev. Mol. Cell. Biol. **6:**9–20.
43. **Pickart, C. M., and R. E. Cohen.** 2004. Proteasomes and their kin: proteases in the machine age. Nat. Rev. Mol. Cell. Biol. **5:**177–187.
44. **Pintard, L., T. Kurz, S. Glaser, J. H. Willis, M. Peter, and B. Bowerman.** 2003. Neddylation and Deneddylation of CUL-3 is required to target MEI-1/katanin for degradation at the meiosis-to-mitosis transition in *C. elegans*. Curr. Biol. **13:**911–921.
45. **Pintard, L., A. Willems, and M. Peter.** 2004. Cullin-based ubiquitin ligases: Cul3-BTB complexes join the family. EMBO J. **23:**1681–1687.
46. **Pintard, L., J. H. Willis, A. Willems, J. L. Johnson, M. Srayko, T. Kurz, S. Glaser, P. E. Mains, M. Tyers, B. Bowerman, and M. Peter.** 2003. The BTB protein MEL-26 is a substrate-specific adaptor of the CUL-3 ubiquitin-ligase. Nature **425:**311–316.
47. **Polanowska, J., J. S. Martin, R. Fisher, T. Scopa, I. Rae, and S. J. Boulton.** 2004. Tandem immunoaffinity purification of protein complexes from *Caenorhabditis elegans*. BioTechniques **36:**778–780, 782.
48. **Sambrook, J., E. F. Fristch, and T. Maniatis.** 1989. Molecular cloning: a laboratory manual, 2nd ed. Cold Spring Harbor Laboratory Press, Cold Spring harbor, NY.
49. **Schwechheimer, C., G. Serino, J. Callis, W. L. Crosby, S. Lyapina, R. J. Deshaies, W. M. Gray, M. Estelle, and X. W. Deng.** 2001. Interactions of the COP9 signalosome with the E3 ubiquitin ligase SCFTIRI in mediating auxin response. Science **292:**1379–1382.
50. **Shalev, A., L. Valasek, C. A. Pise-Masison, M. Radonovich, L. Phan, J. Clayton, H. He, J. N. Brady, A. G. Hinnebusch, and K. Asano.** 2001. *Saccharomyces cerevisiae* protein Pci8p and human protein eIF3e/Int-6 interact with the eIF3 core complex by binding to cognate eIF3b subunits. J. Biol. Chem. **276:**34948–34957.
51. **Sonnichsen, B., L. B. Koski, A. Walsh, P. Marschall, B. Neumann, M. Brehm, A. M. Alleaume, J. Artelt, P. Bettencourt, E. Cassin, M. Hewitson, C. Holz, M. Khan, S. Lazik, C. Martin, B. Nitzsche, M. Ruer, J. Stamford, M. Winzi, R. Heinkel, M. Roder, J. Finell, H. Hantsch, S. J. Jones, M. Jones, F. Piano, K. C. Gunsalus, K. Oegema, P. Gonczy, A. Coulson, A. A. Hyman, and C. J. Echeverri.** 2005. Full-genome RNAi profiling of early embryogenesis in *Caenorhabditis elegans*. Nature **434:**462–469.
52. **Srayko, M., D. W. Buster, O. A. Bazirgan, F. J. McNally, and P. E. Mains.** 2000. MEI-1/MEI-2 katanin-like microtubule severing activity is required for *Caenorhabditis elegans* meiosis. Genes Dev. **14:**1072–1084.
53. **Srayko, M., T. O'Toole, E. A. A. Hyman, and T. Muller-Reichert.** 2006. Katanin disrupts the microtubule lattice and increases polymer number in *C. elegans* meiosis. Curr. Biol. **16:**1944–1949.
54. **Sugasawa, K., Y. Okuda, M. Saijo, R. Nishi, N. Matsuda, G. Chu, T. Mori, S. Iwai, K. Tanaka, and F. Hanaoka.** 2005. UV-induced ubiquitylation of XPC protein mediated by UV-DDB-ubiquitin ligase complex. Cell **121:**387–400.
55. **Thompson, J. D., D. G. Higgins, and T. J. Gibson.** 1994. CLUSTAL W: improving the sensitivity of progressive multiple sequence alignment through sequence weighting, position-specific gap penalties and weight matrix choice. Nucleic Acids Res. **22:**4673–4680.
56. **Unbehaun, A., S. I. Borukhov, C. U. Hellen, and T. V. Pestova.** 2004. Release of initiation factors from 48S complexes during ribosomal subunit joining and the link between establishment of codon-anticodon base-pairing and hydrolysis of eIF2-bound GTP. Genes Dev. **18:**3078–3093.
57. **Verma, R., L. Aravind, R. Oania, W. H. McDonald, J. R. Yates III, E. V. Koonin, and R. J. Deshaies.** 2002. Role of Rpn11 metalloprotease in deubiquitination and degradation by the 26S proteasome. Science **298:**611–615.
58. **Wee, S., R. K. Geyer, T. Toda, and D. A. Wolf.** 2005. CSN facilitates Cullin-RING ubiquitin ligase function by counteracting autocatalytic adapter instability. Nat. Cell Biol. **7:**387–391.
59. **Wei, N., D. A. Chamovitz, and X. W. Deng.** 1994. Arabidopsis COP9 is a component of a novel signaling complex mediating light control of development. Cell **78:**117–124.
60. **Wei, N., and X. W. Deng.** 2003. The COP9 signalosome. Annu. Rev. Cell Dev. Biol. **19:**261–286.
61. **Wei, W., N. G. Ayad, Y. Wan, G. J. Zhang, M. W. Kirschner, and W. G. Kaelin, Jr.** 2004. Degradation of the SCF component Skp2 in cell-cycle phase $G_1$ by the anaphase-promoting complex. Nature **428:**194–198.
62. **Willems, A. R., M. Schwab, and M. Tyers.** 2004. A hitchhiker's guide to the cullin ubiquitin ligases: SCF and its kin. Biochim. Biophys. Acta **1695:**133–170.
63. **Wu, J. T., H. C. Lin, Y. C. Hu, and C. T. Chien.** 2005. Neddylation and deneddylation regulate Cul1 and Cul3 protein accumulation. Nat. Cell Biol. **7:**1014–1020.
64. **Xu, L., Y. Wei, J. Reboul, P. Vaglio, T. H. Shin, M. Vidal, S. J. Elledge, and J. W. Harper.** 2003. BTB proteins are substrate-specific adaptors in an SCF-like modular ubiquitin ligase containing CUL-3. Nature **425:**316–321.
65. **Yen, H. C., C. Gordon, and E. C. Chang.** 2003. *Schizosaccharomyces pombe Int6* and *Ras* homologs regulate cell division and mitotic fidelity via the proteasome. Cell **112:**207–217.
66. **Zheng, J., X. Yang, J. M. Harrell, S. Ryzhikov, E. H. Shim, K. Lykke-Andersen, N. Wei, H. Sun, R. Kobayashi, and H. Zhang.** 2002. CAND1 binds to unneddylated CUL1 and regulates the formation of SCF ubiquitin E3 ligase complex. Mol. Cell **10:**1519–1526.
67. **Zheng, N., B. A. Schulman, L. Song, J. J. Miller, P. D. Jeffrey, P. Wang, C. Chu, D. M. Koepp, S. J. Elledge, M. Pagano, R. C. Conaway, J. W. Conaway, J. W. Harper, and N. P. Pavletich.** 2002. Structure of the Cul1-Rbx1-Skp1-F boxSkp2 SCF ubiquitin ligase complex. Nature **416:**703–709.
68. **Zhou, C., F. Arslan, S. Wee, S. Krishnan, A. R. Ivanov, A. Oliva, J. Leatherwood, and D. A. Wolf.** 2005. PCI proteins eIF3e and eIF3m define distinct translation initiation factor 3 complexes. BMC Biol. **3:**14.
69. **Zhou, C., S. Wee, E. Rhee, M. Naumann, W. Dubiel, and D. A. Wolf.** 2003. Fission yeast CSN suppresses cullin activity through recruitment of the deubiquitylating enzyme Ubp12p. Mol. Cell **11:**927–938.